



Characterization of CNM's 3D pixel sensors for the CMS Phase-2 upgrade

23rd RD50 Workshop
CERN, 15th October 2013

Francisca Muñoz (IFCA)
fjmunoz@ifca.unican.es



M. Lozano
G. Pellegrini
D. Quirion



E. Currás, M. Fernández
G. Gómez, R. Jaramillo
F.J. Muñoz, I. Vila



T. Rohe



D. Hits
M. Rossini



D. Pitzl
S. Spannagel

Outline

- Motivation
- 3D pixel technology and manufacturing
- Electrical characterization
- PSI46 Read Out Chip (ROC) and interconnection process
- Radiation resistance studies
- Test Beam Results
- Conclusions

Motivation: LHC to HL-LH

- Luminosity: $10^{34} \text{ cm}^{-2}\text{s}^{-1}$.
- Fluence: $6 \times 10^{14} n_{\text{eq}} \text{ cm}^{-2}$.
- Inner Radius: 4.4 cm
- Planar n-on-n sensors



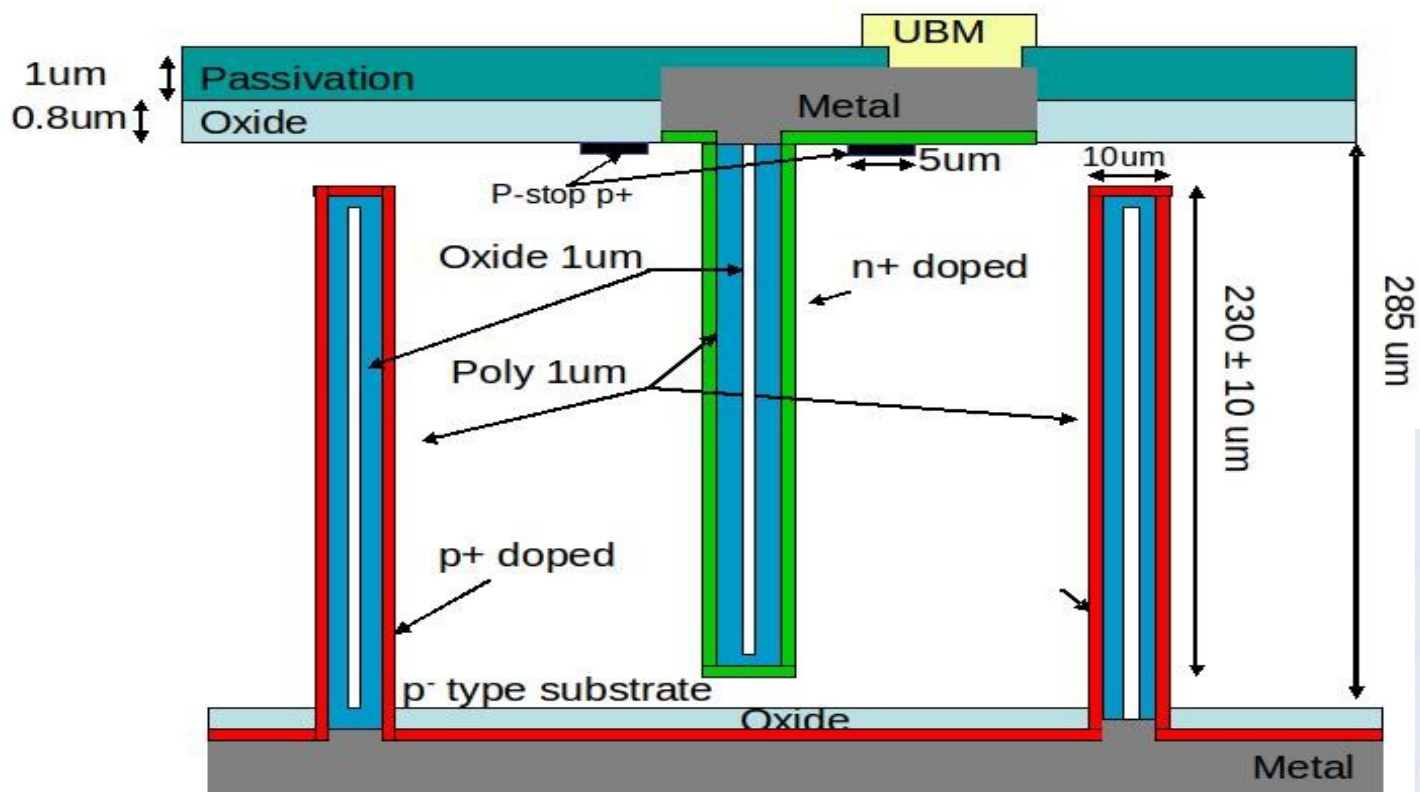
- Luminosity: $10^{35} \text{ cm}^{-2}\text{s}^{-1}$.
- Fluence: $2 \times 10^{16} n_{\text{eq}} \text{ cm}^{-2}$.
- Inner Radius: 3 cm
- 3D, thinned, n-on-p or diamond sensors?

Here we are going to assess the radiation resistance of 3D double-sided pixel sensors in terms of:

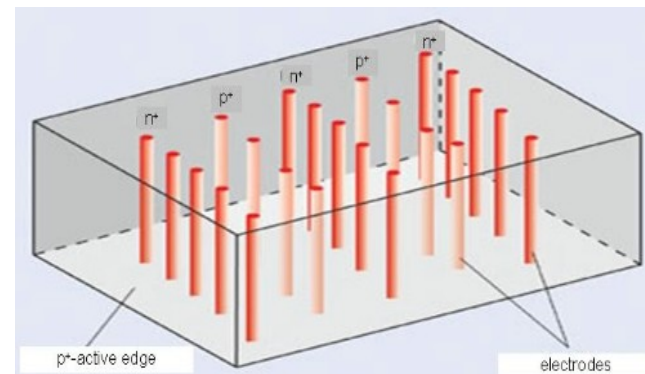
- Increase of the depletion voltage (V_{fd})
- Reduction of the CCE
- Tracking Performance and efficiency

Technology

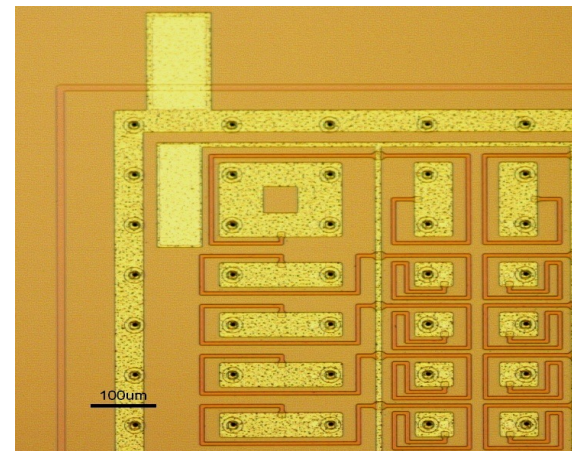
- Double-sided configuration (different doping type on each side)
- Simpler fabrication process
- Photo-lithography to define electrode contacts is only necessary on top surface
- HV biasing on the back side by simple wire bonding



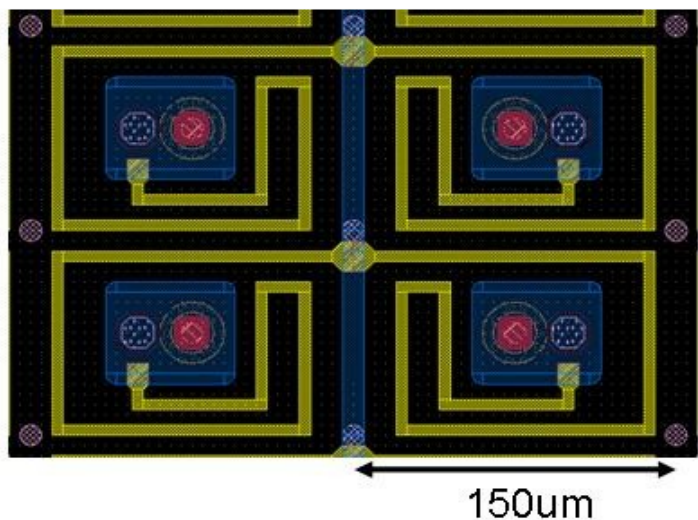
Proposed by G. Pellegrini
(2006)



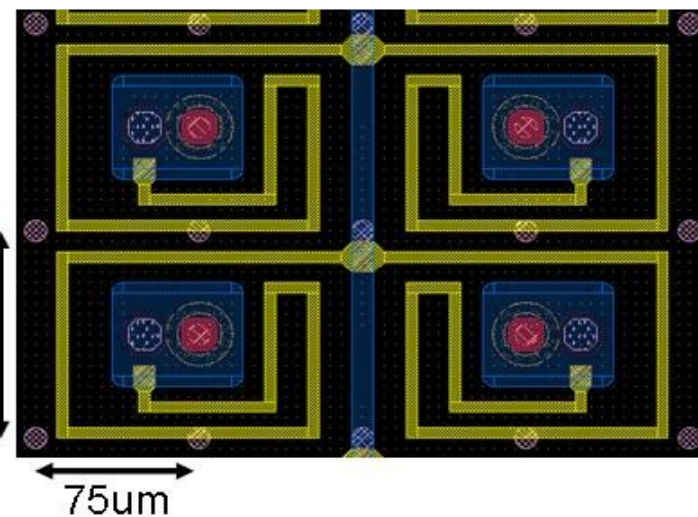
Sensor layout



- * In the back side, two columns pattern.
 - Dense → reduced drift distance
Expected higher radiation resistance
 - Sparse → larger drift distance
Expected lower noises (lower capacitance)



Sparse pattern of holes P:
Rectangular matrix of 150x100um²



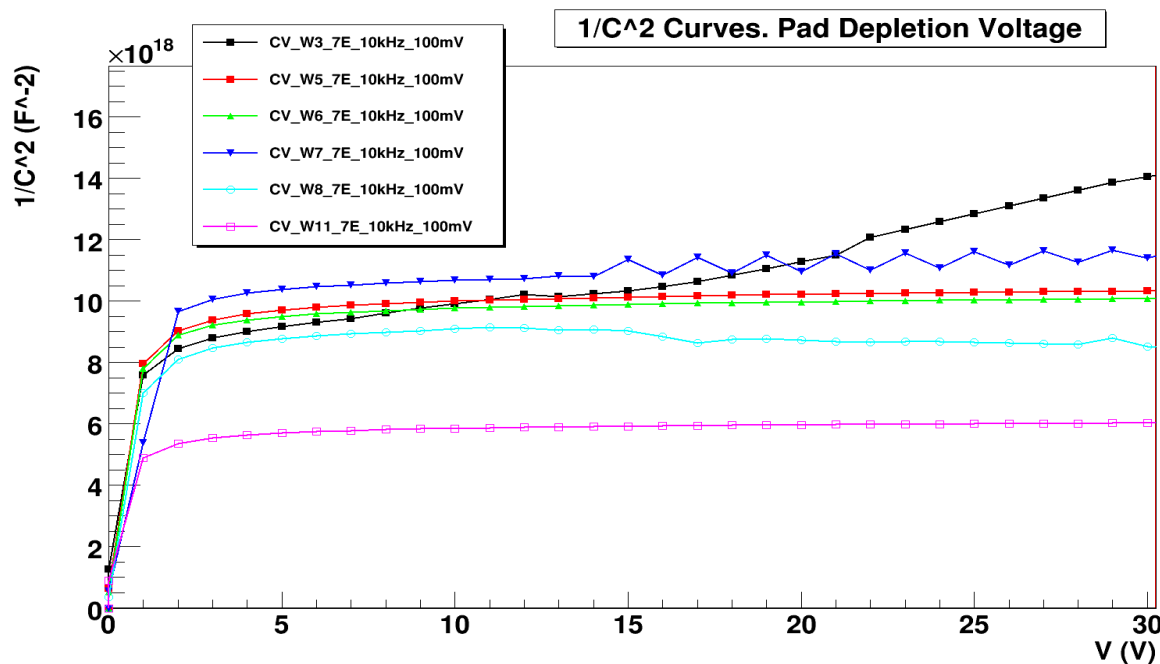
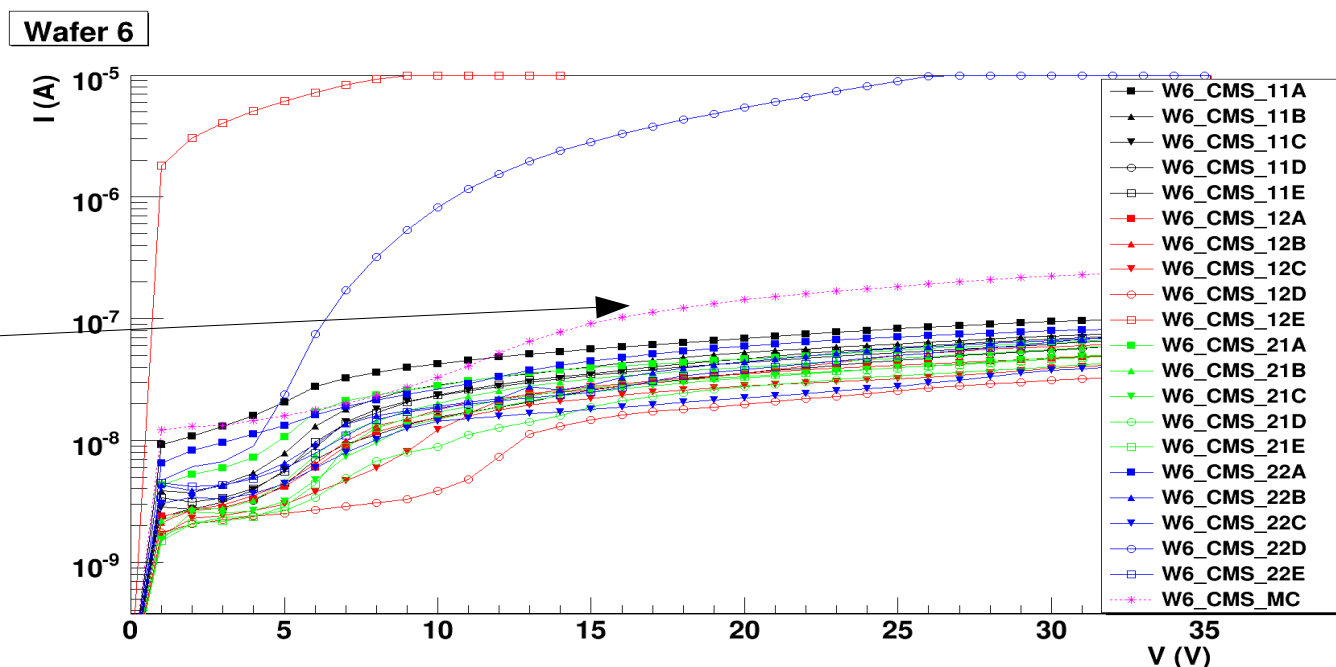
Dense pattern of holes P:
Rectangular matrix of 75x100um²

*** Wafer with a polysilicon resistor implemented for biasing without ROC**

Electrical characterization

IV Curves:
20 Single Chips with different Geometries.
1 CMS Full Module.

High homogeneity
And
Low current values



Vfd measured in
dedicated TS.
Pads.

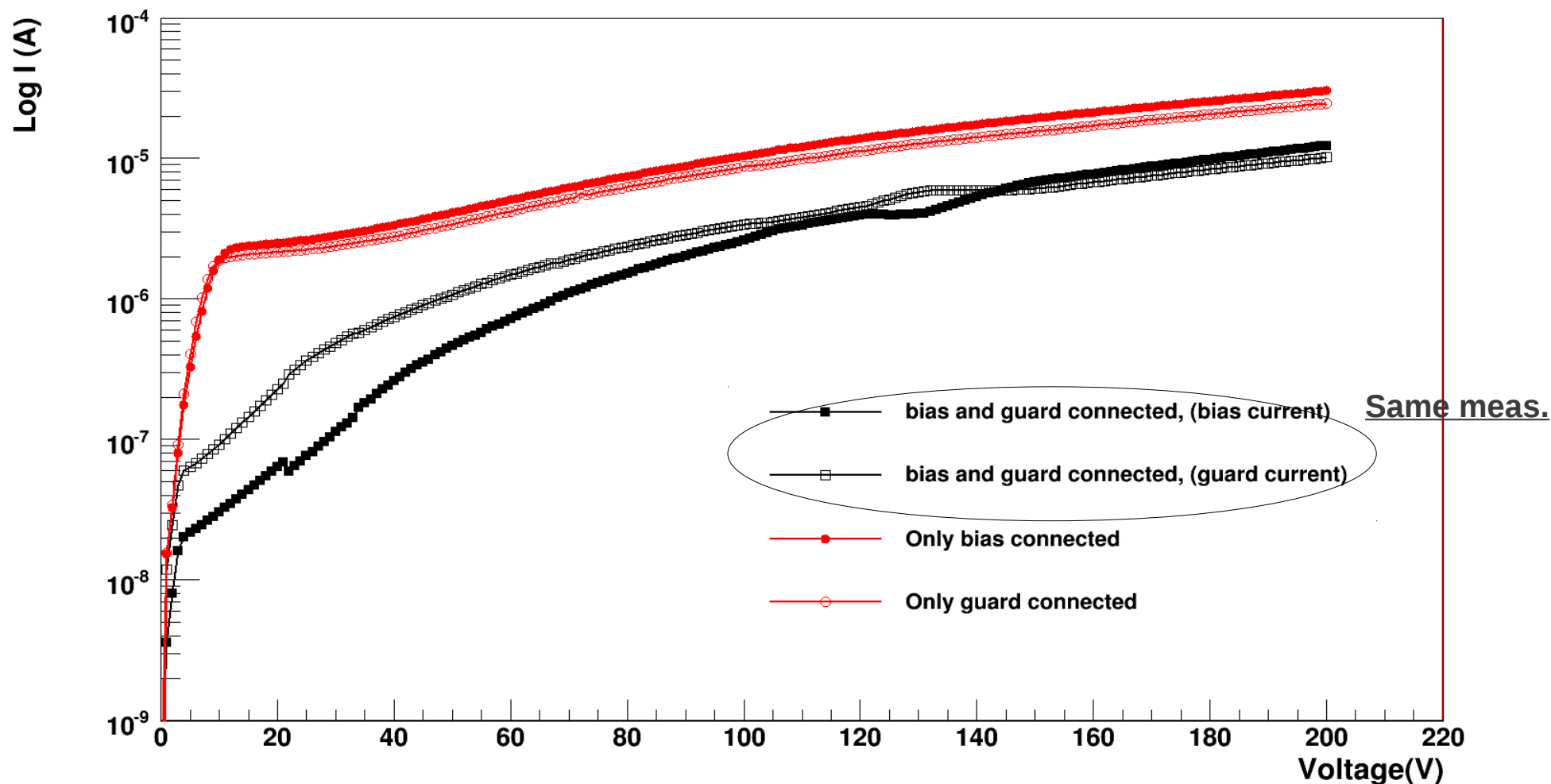
Vfd (3D-Detector) ~ 9 V

Biassing studies

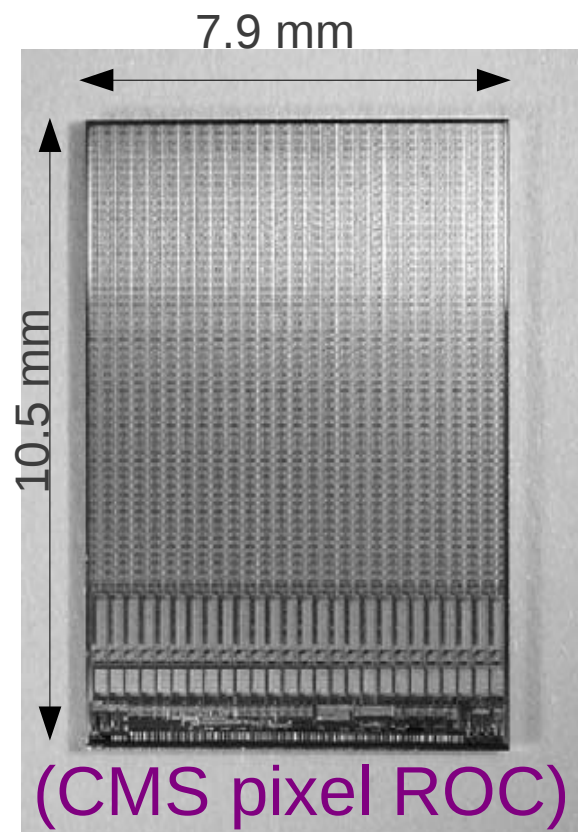
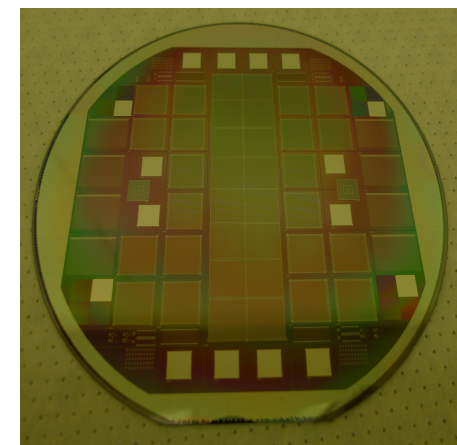


Only guard connected → “punch through” polarization
Only bias connected → pixel by pixel polarization

biassing studies. Detector 12B

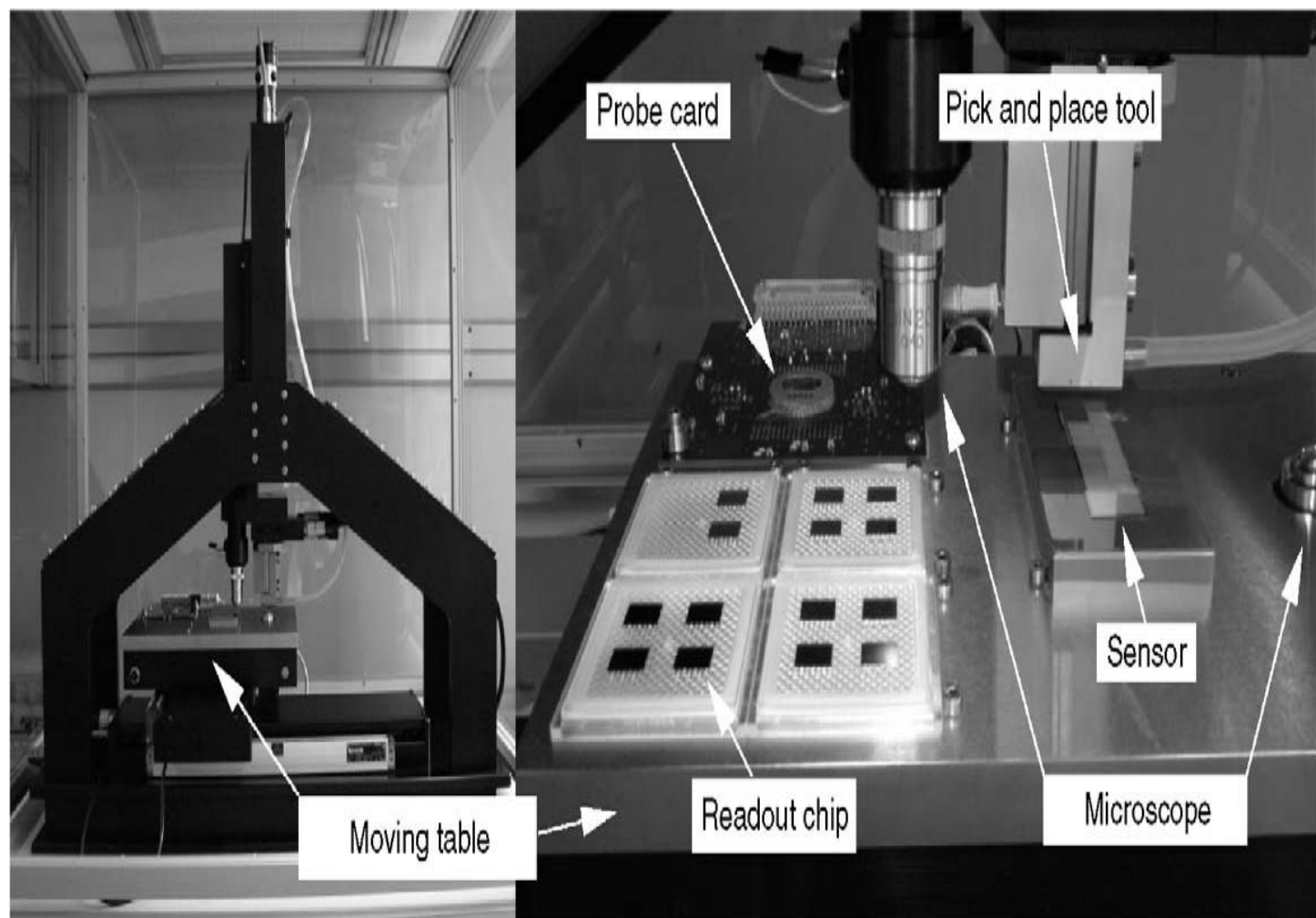


PSI46 ROC and interconnection process

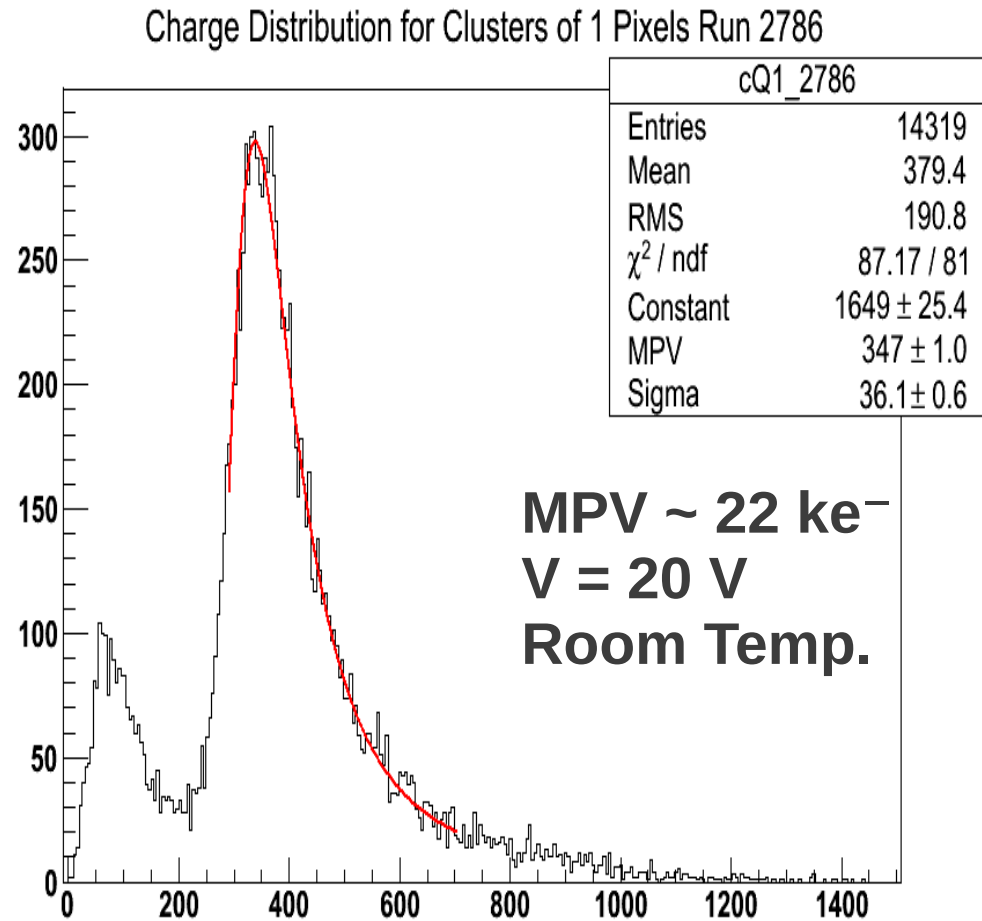
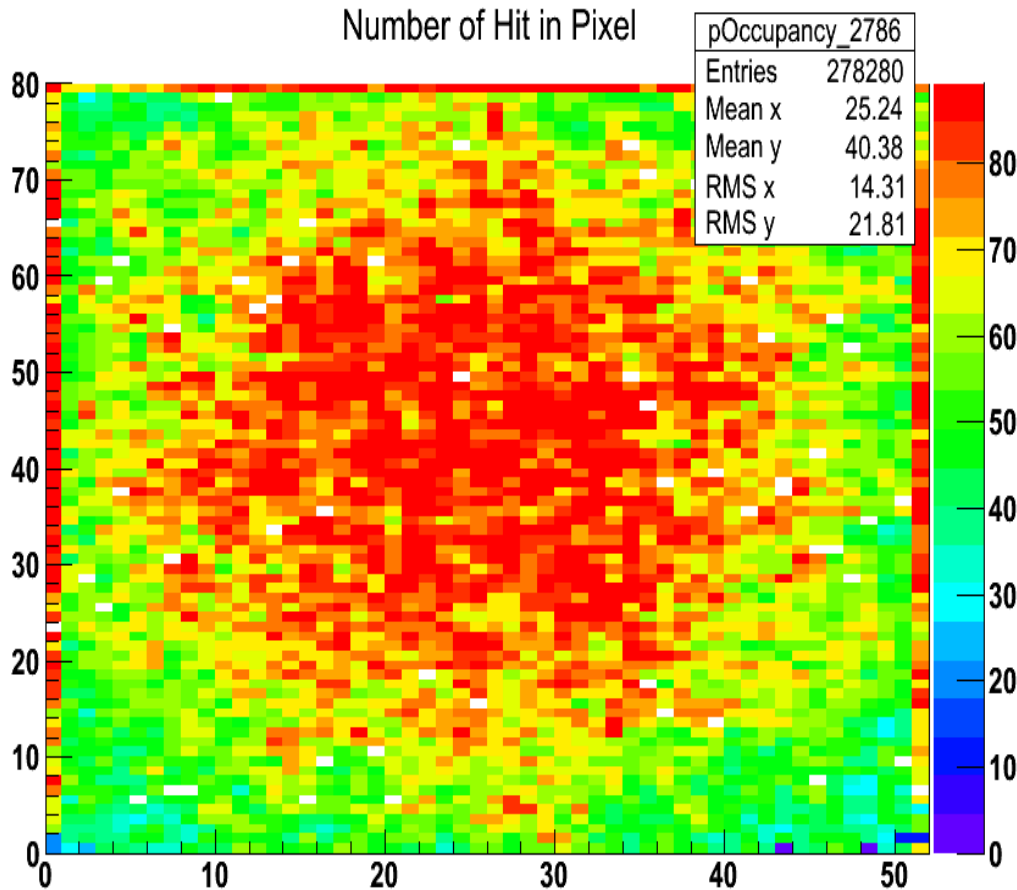


52 x 80 pixel unit cells.
4160 units
150 μ m x 150 μ m

fjmunoz@ifca.unican.es



Nice Pixel map, and landau fit:



Irradiation Campaign:

4 pixel samples, 2 strips detectors and 2 pads up to each radiation fluence

- Proton Cyclotron @ KIT (Karlsruhe), 25MeV protons:

$$1 \times 10^{15} n_{eq}/cm^2$$

$$5 \times 10^{15} n_{eq}/cm^2$$

- Tigra Reactor @ JSI (Ljubljana), continuous spectrum neutrons:

$$1 \times 10^{15} n_{eq}/cm^2$$

$$5 \times 10^{15} n_{eq}/cm^2$$

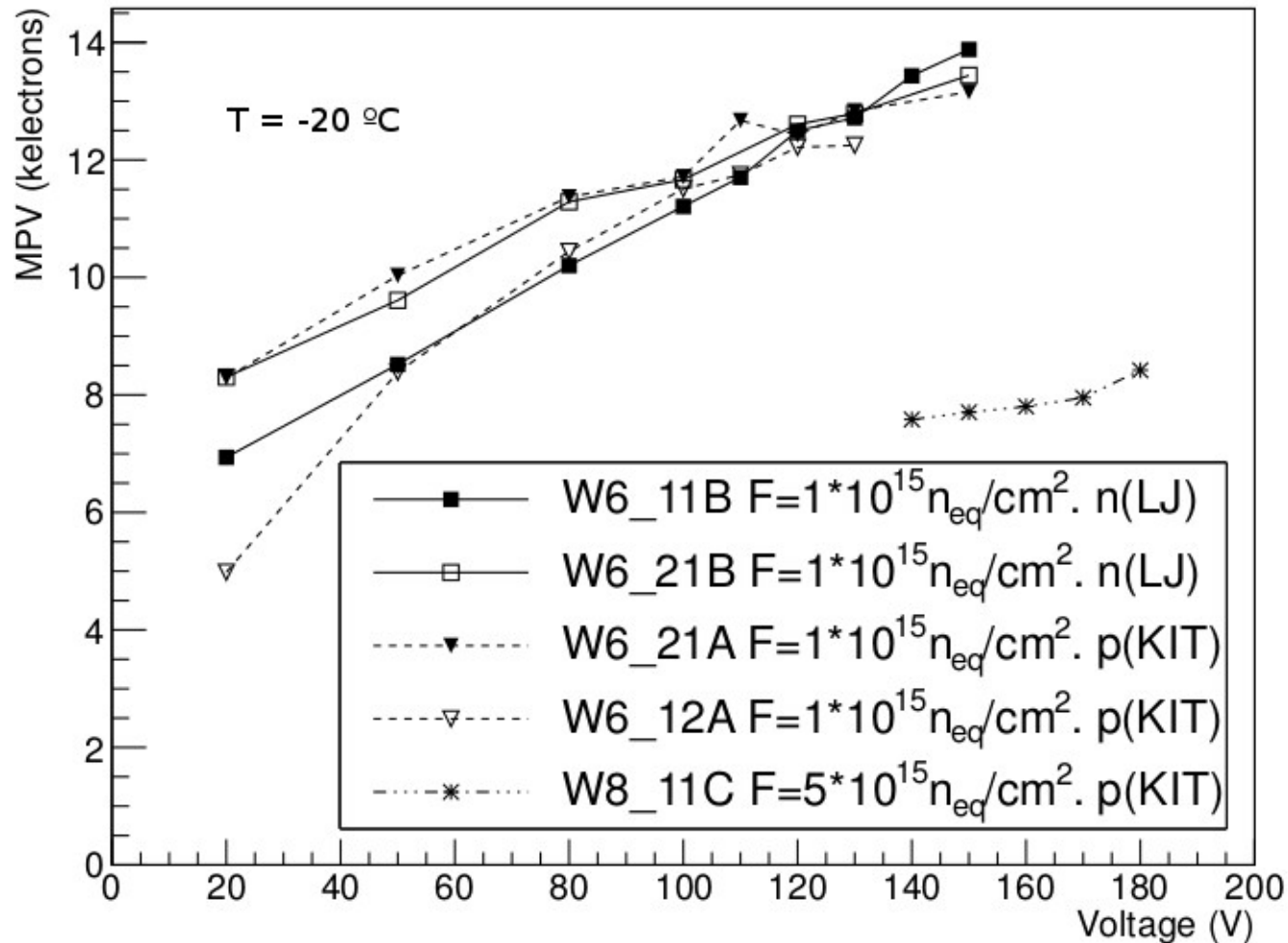
$$1 \times 10^{16} n_{eq}/cm^2$$

^{90}Sr Characterization

- * **Charge Collection in irradiated samples**
- * **Full Depletion Voltage:**
 - Depletion Area grows in a 3D sensor horizontally
 - A new variable:

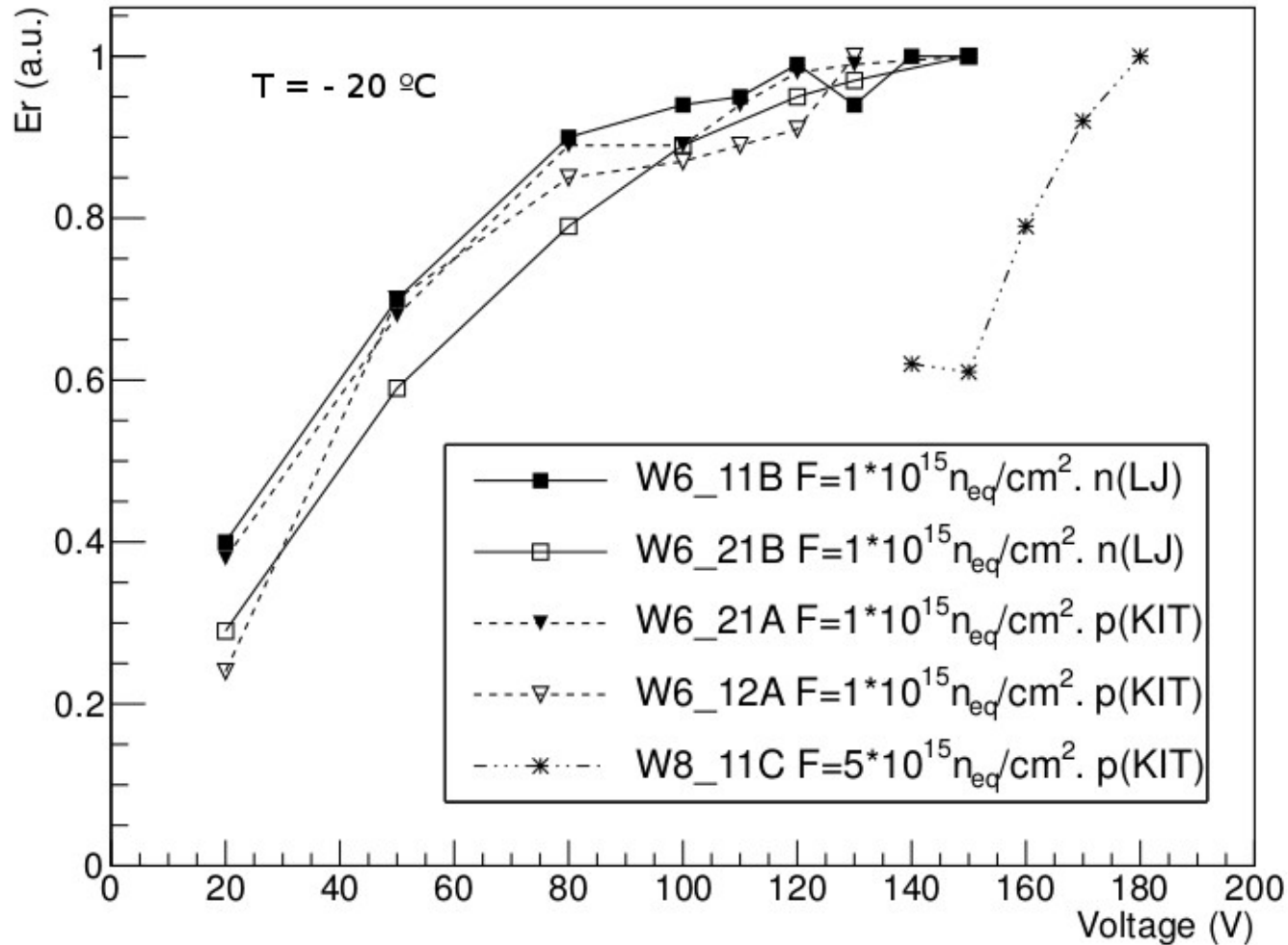
$$E_r = \frac{\text{Num. of hits}}{\text{Num. of triggers}}$$
 - When the E_r saturates with bias voltage, we consider that we have depleted the maximum volume in the sensor

MPV vs bias Voltage in irradiated samples



NIM A: <http://www.sciencedirect.com/science/article/pii/S0168900213007328>

Er vs bias Voltage in irradiated samples

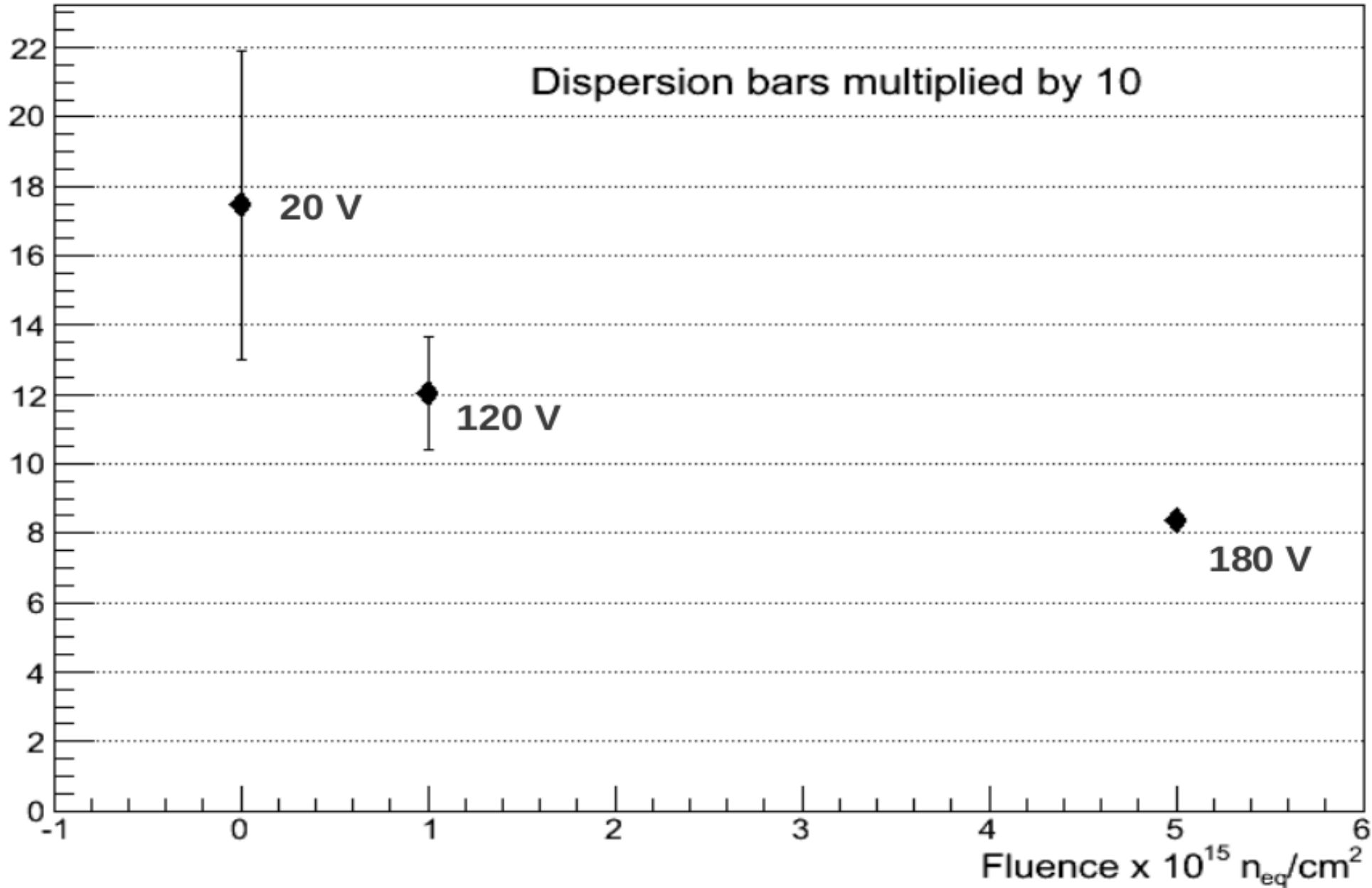


NIM A: <http://www.sciencedirect.com/science/article/pii/S0168900213007328>

Summary after ^{90}Sr characterization

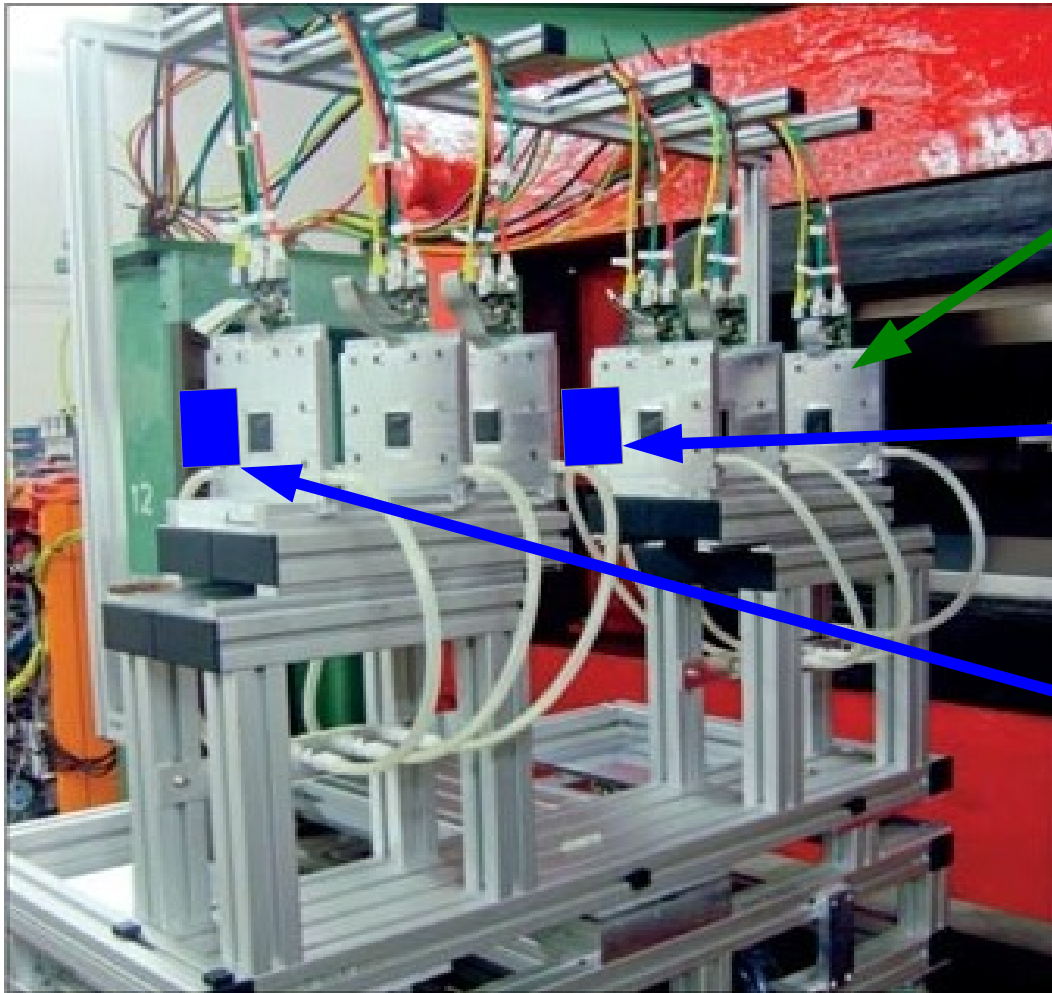


MPV kelectrons



DESY TEST BEAM.

e^+ beam (6 GeV)



DESY Experimental area 21:

DATURA TELESCOPE:

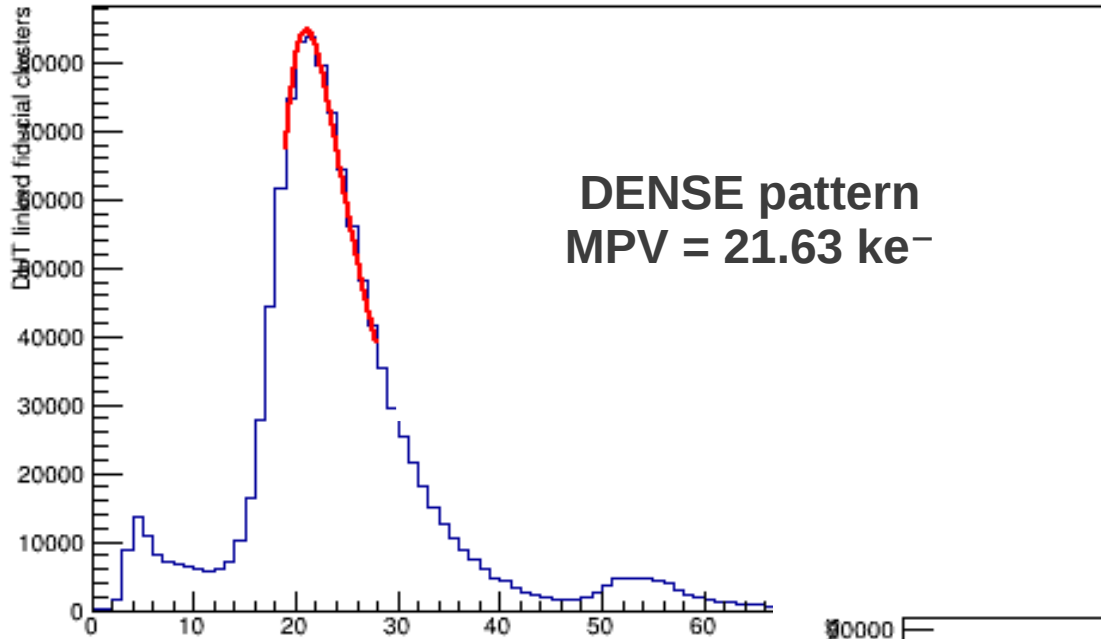
- 6 Mimosa26 monolithic active pixel sensors (Strasbourg, 2009).

- Device under test (DUT). 3D pixel sensor. Normal incidence.

- Timing reference sensor. Planar CMS sensor, to correct telescope pile-up.

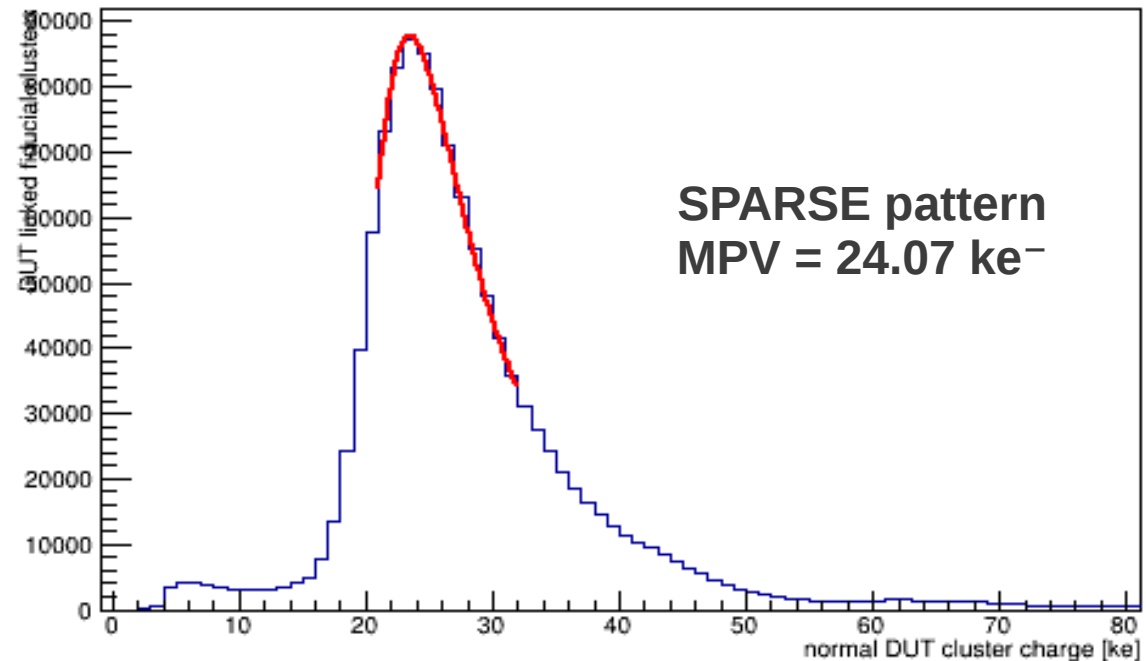
TEST BEAM RESULTS.

Unirradiated sensors.



Charge distribution differences
Can be due to:
ROC calibration uncertainties
that can be about 15 %.
Not necessary to the different
patterns

$V_{\text{bias}} = 20 \text{ V}$
Room Temp.



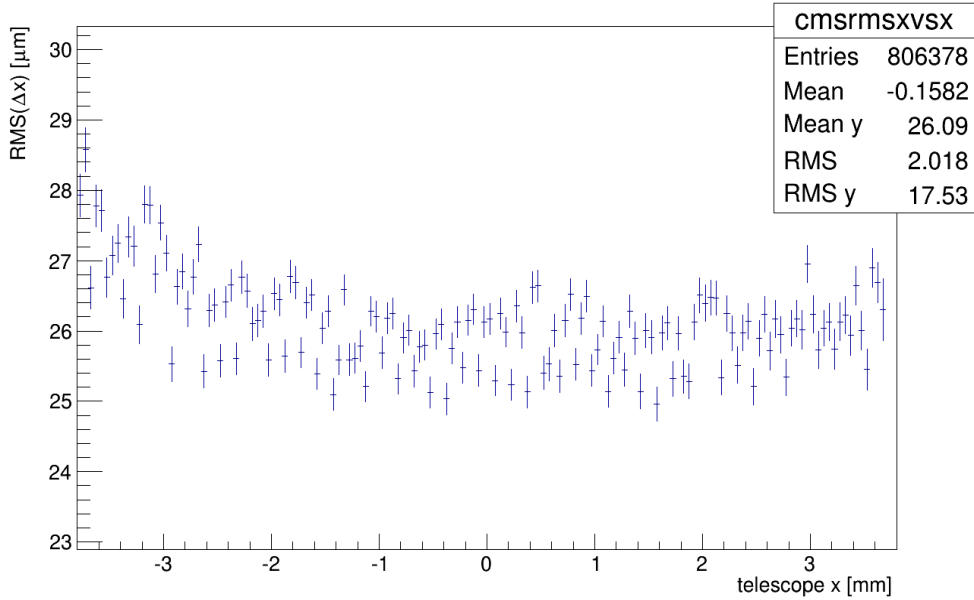
Resolution. Unirradiated Samples

Dense

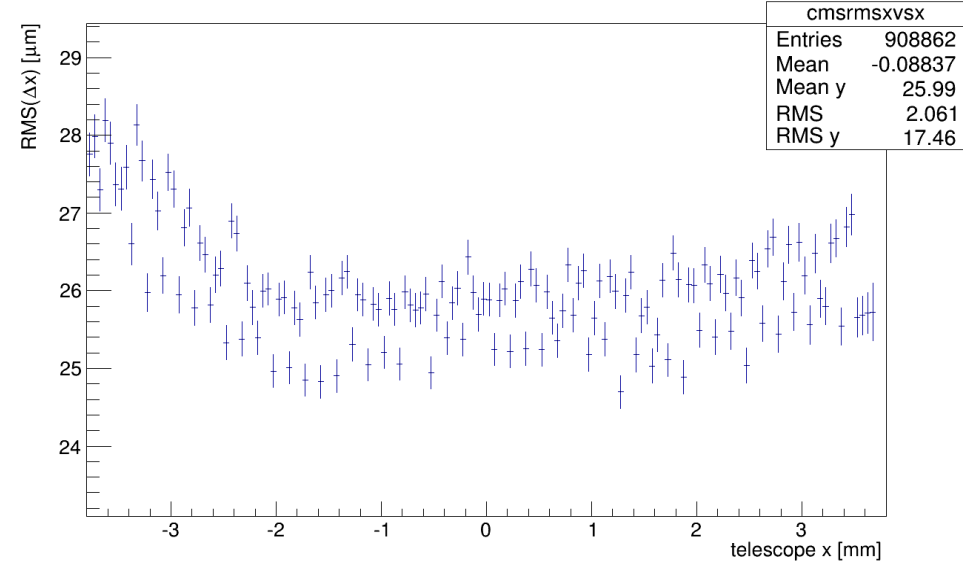
$$100/\sqrt{12} = 28 \text{ } \mu\text{m}$$

Sparse

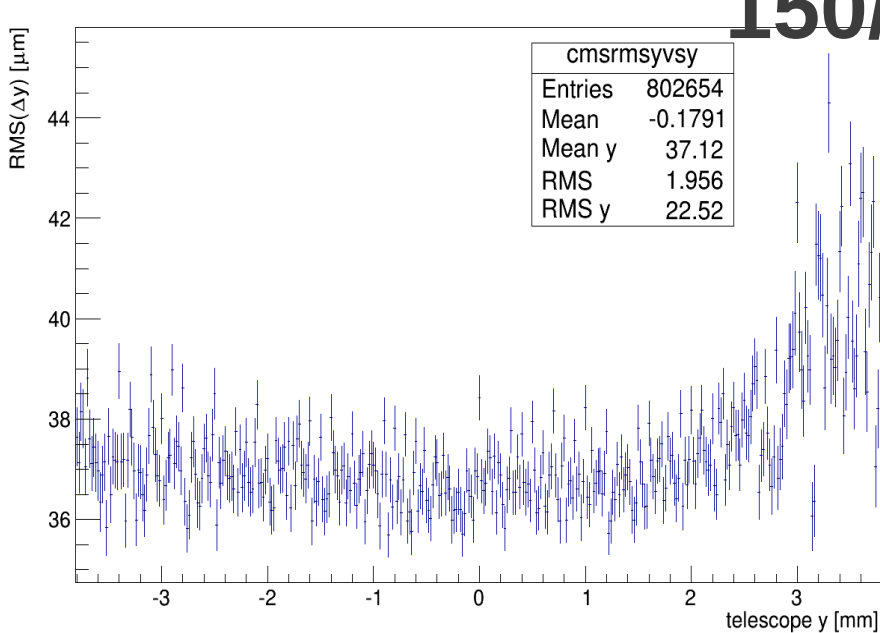
DUT x resolution vs x



DUT x resolution vs x

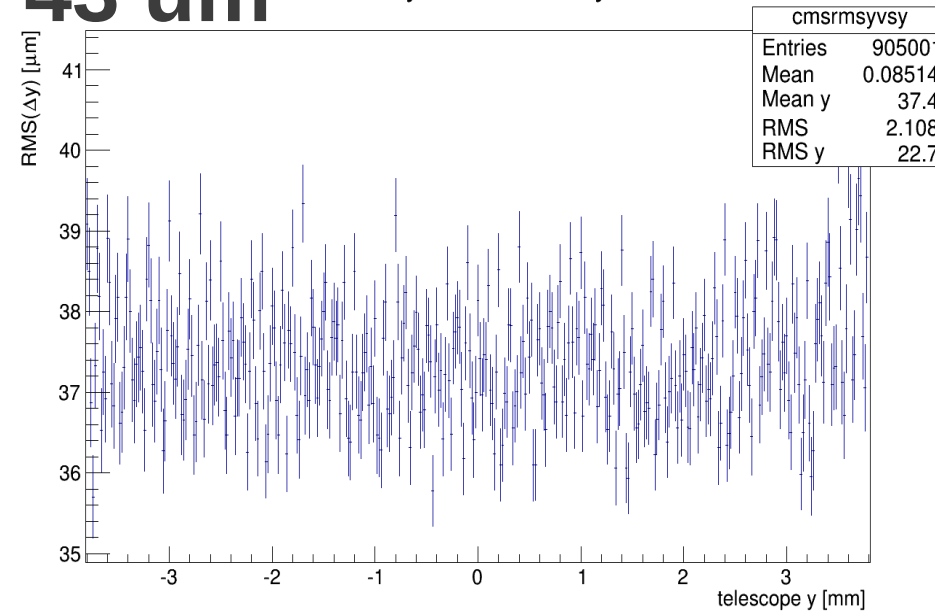


DUT y resolution vs y

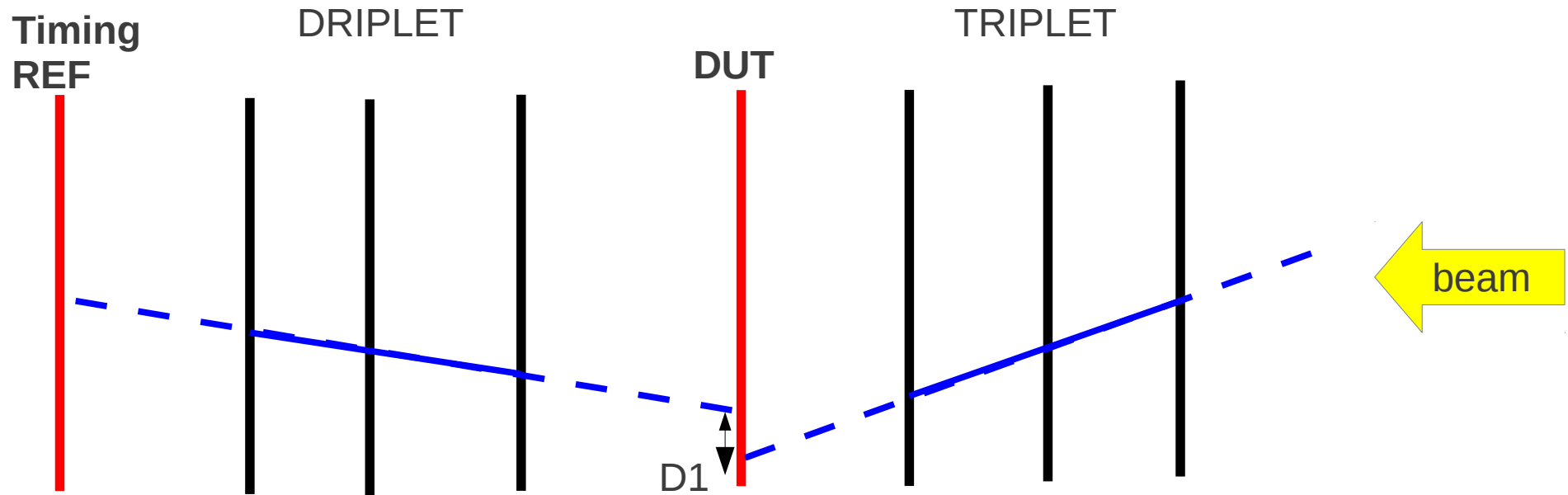


$$150/\sqrt{12} = 43 \text{ } \mu\text{m}$$

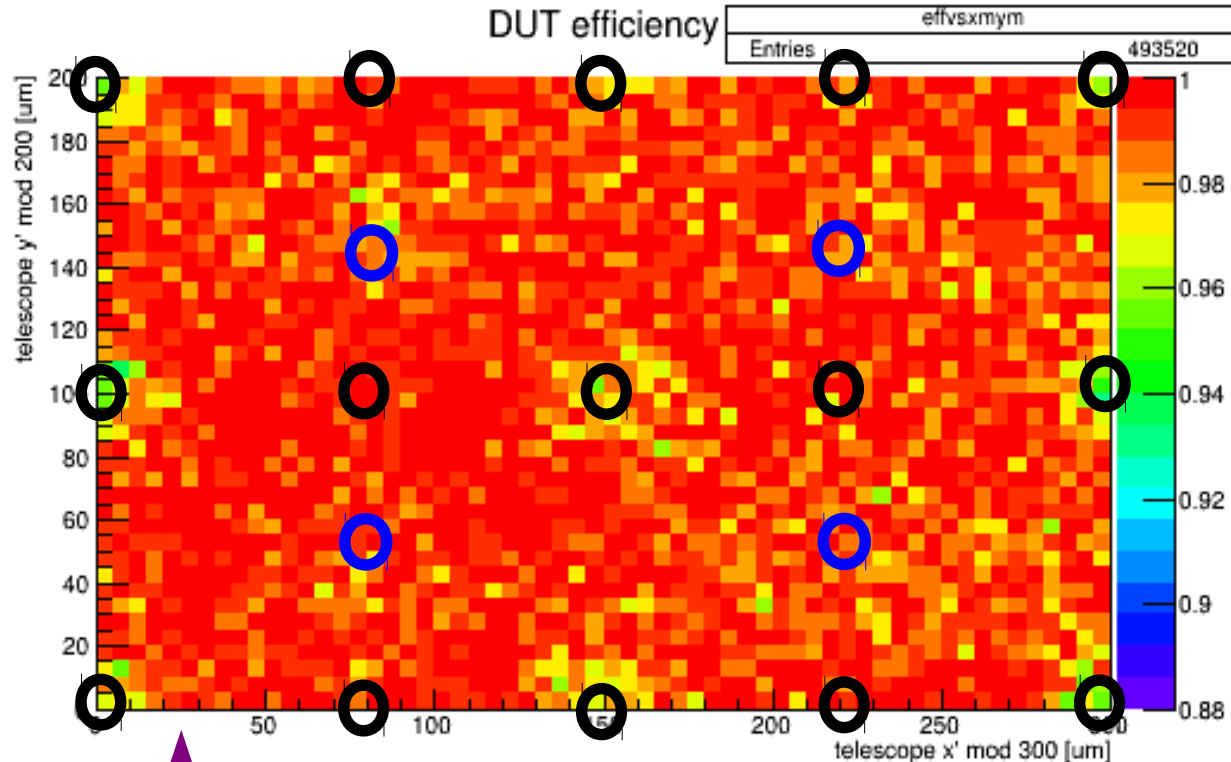
DUT y resolution vs y



Efficiency Tracks selection



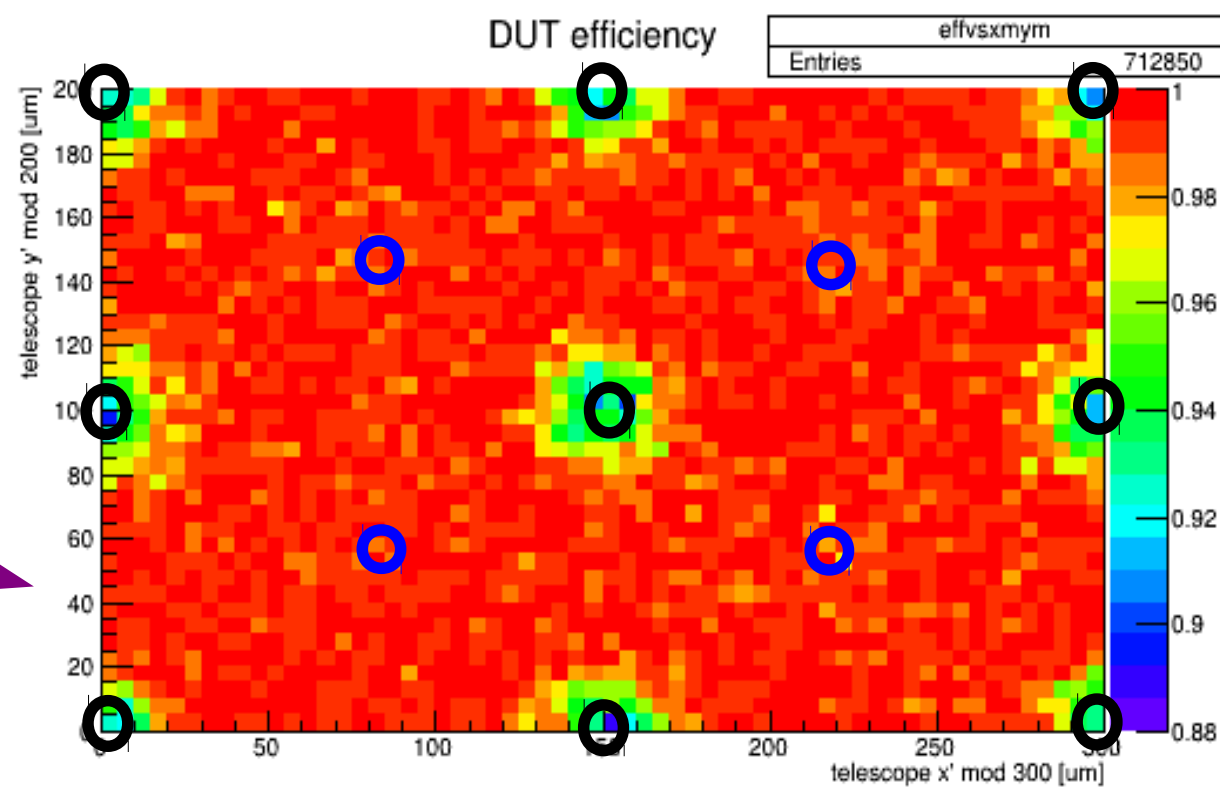
TRACKS: Driplet linked to REF and DUT
Triplet linked to DUT
 $D1 < 500\mu\text{m}$



RESULTS. Unirradiated sensors.

- Pn-junction column
- Ohmic junction column

DENSE pattern sensor shows a more homogeneous behavior in terms of efficiency than sensors with a SPARSE pattern

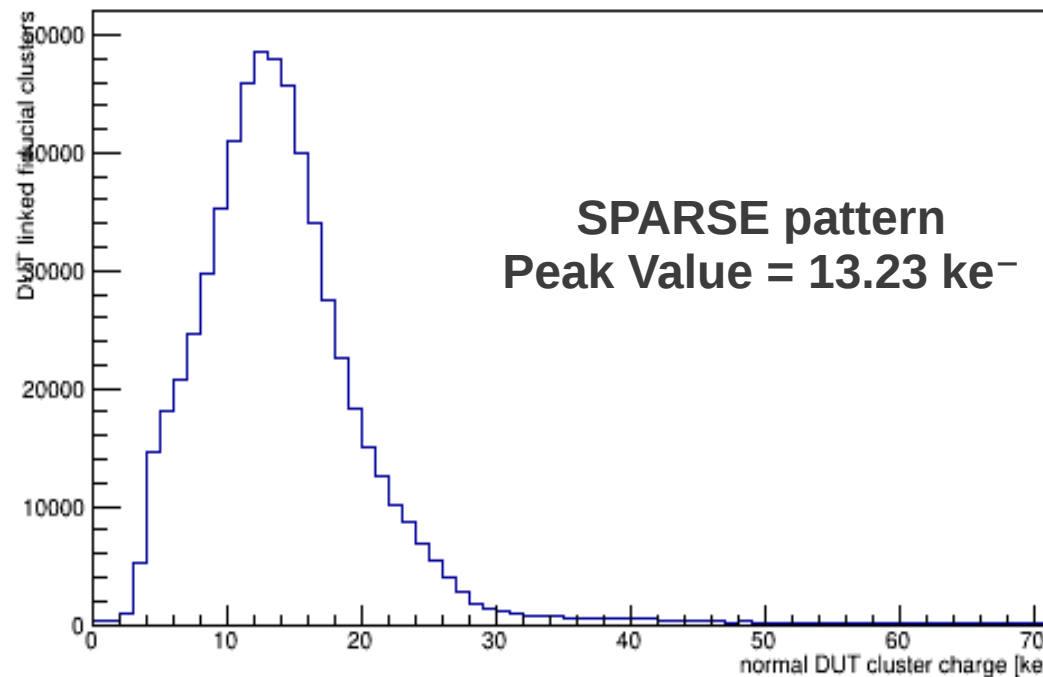
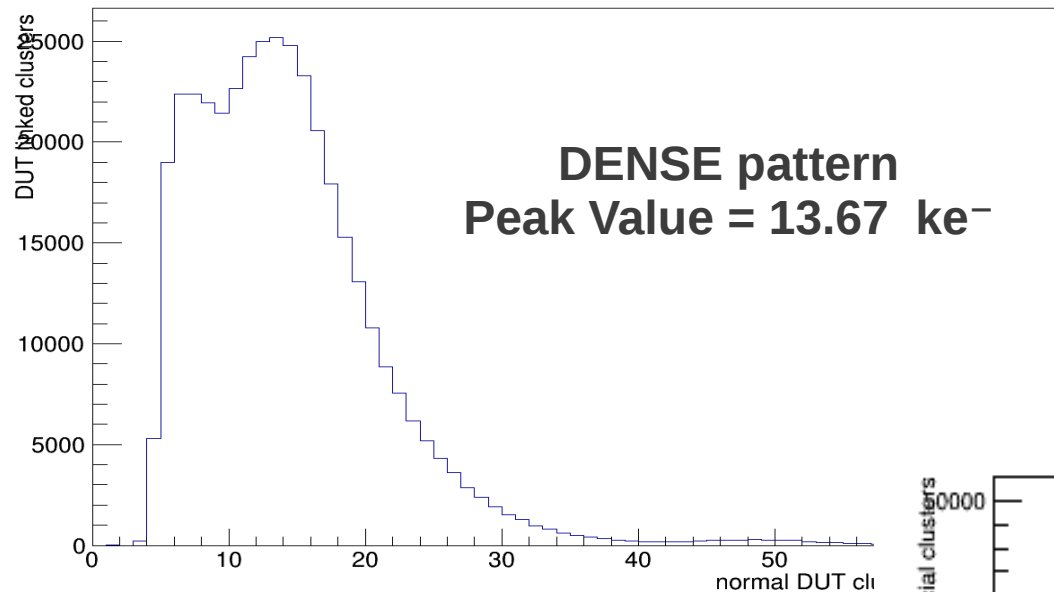


$V_{bias} = 20\text{ V}$
Room Temp.

Fran

TEST BEAM RESULTS.

n- Irradiated sensors ($10^{15} n_{eq}/cm^2$).



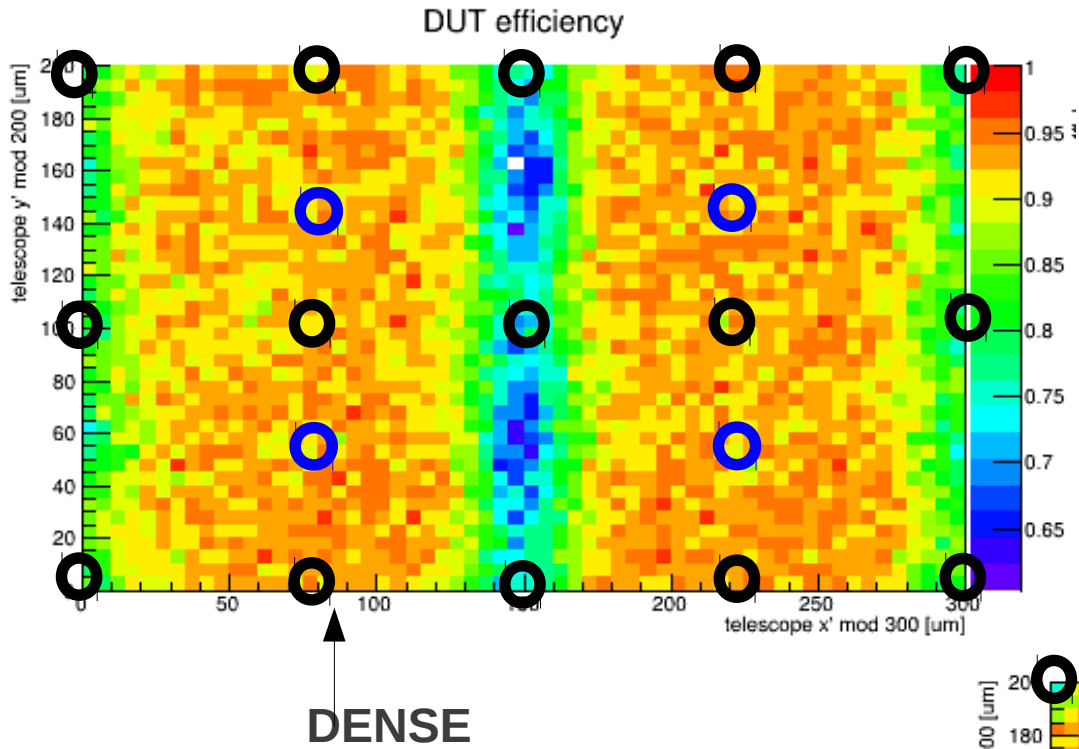
PRELIMINARY

$V_{bias} = 120 V$

$T = -15 \text{ }^\circ\text{C}$

TEST BEAM RESULTS.

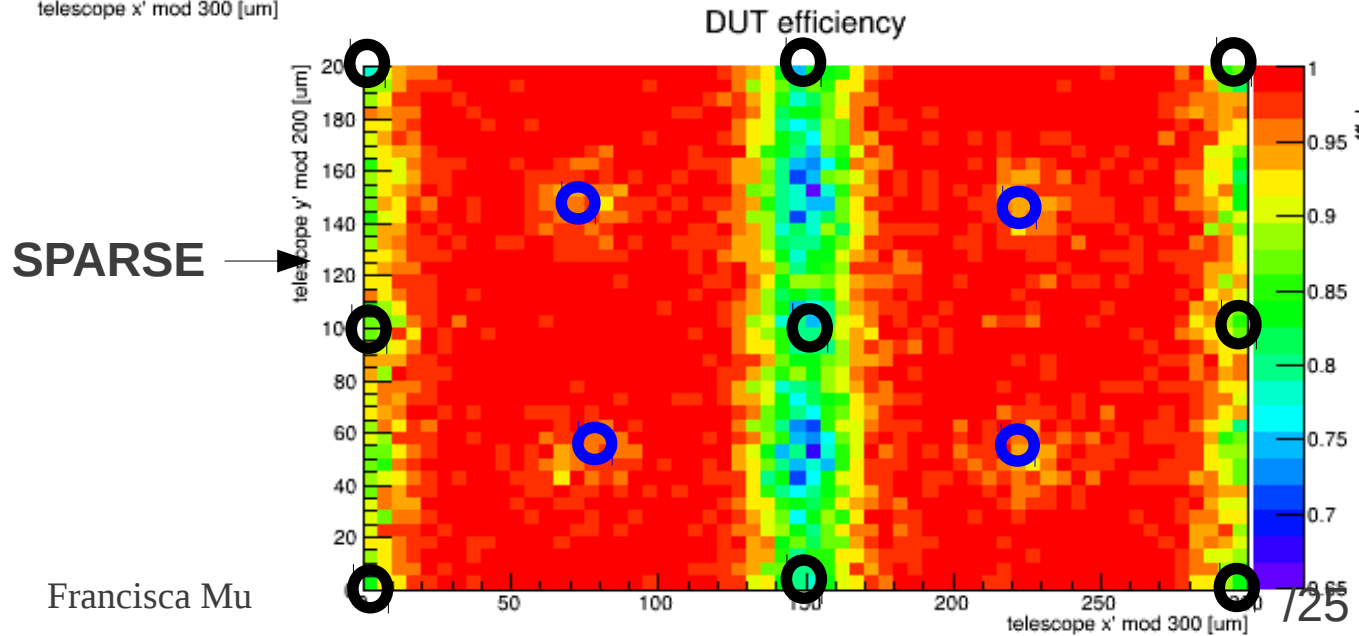
n- Irradiated sensors ($10^{15} n_{eq}/cm^2$).



PRELIMINARY

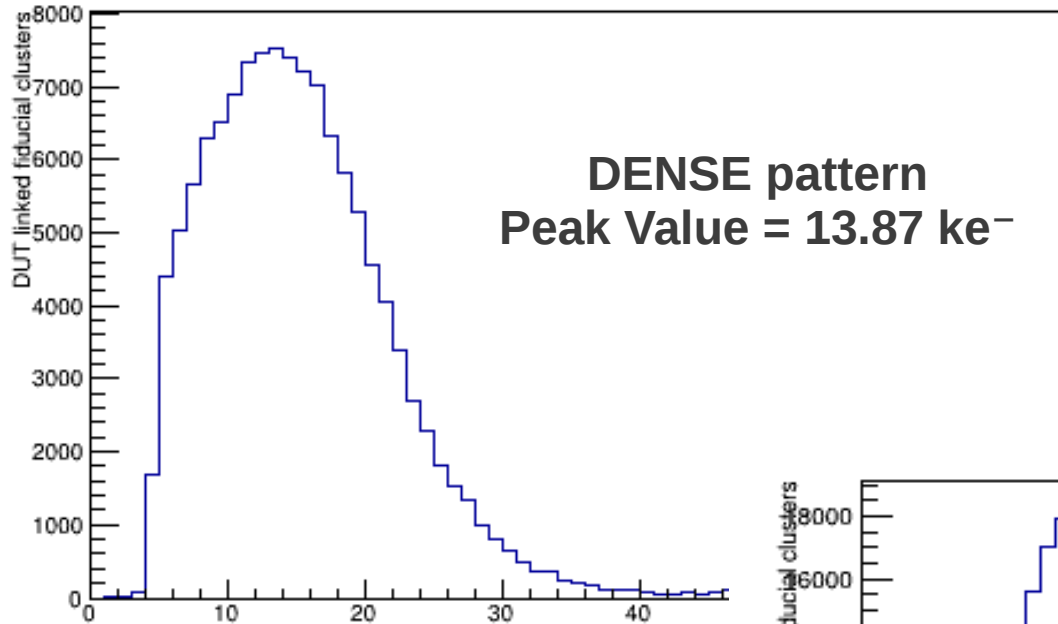
$V_{bias} = 120 V$

$T = -15 ^\circ C$



TEST BEAM RESULTS.

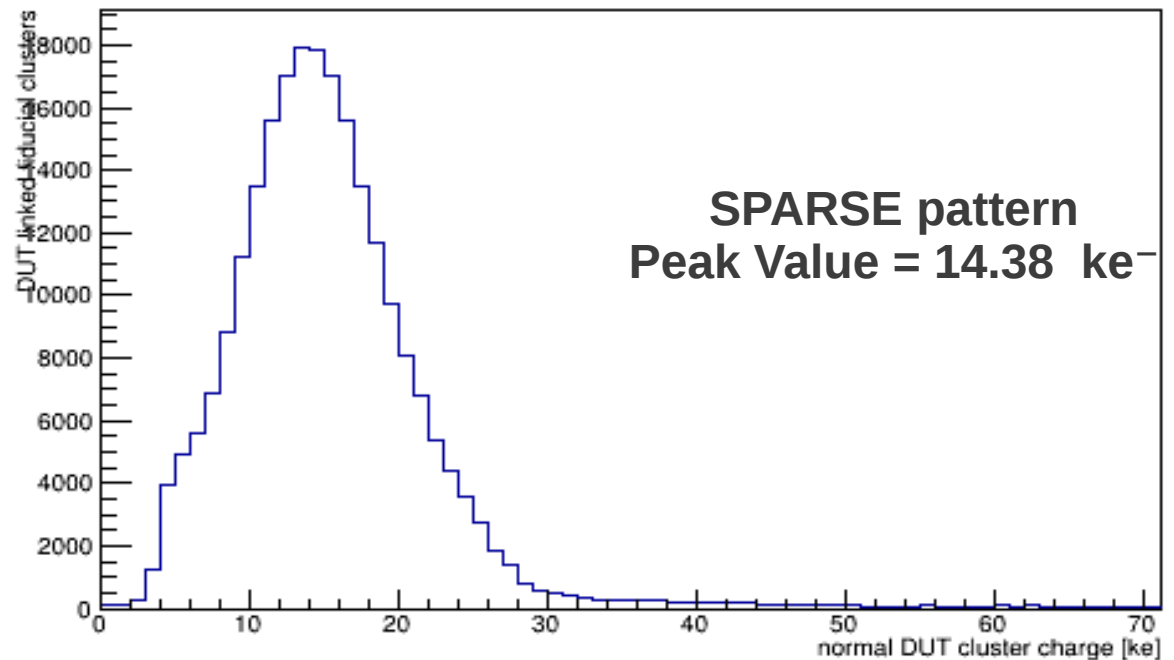
n- Irradiated sensors ($10^{15} n_{eq}/cm^2$).



PRELIMINARY

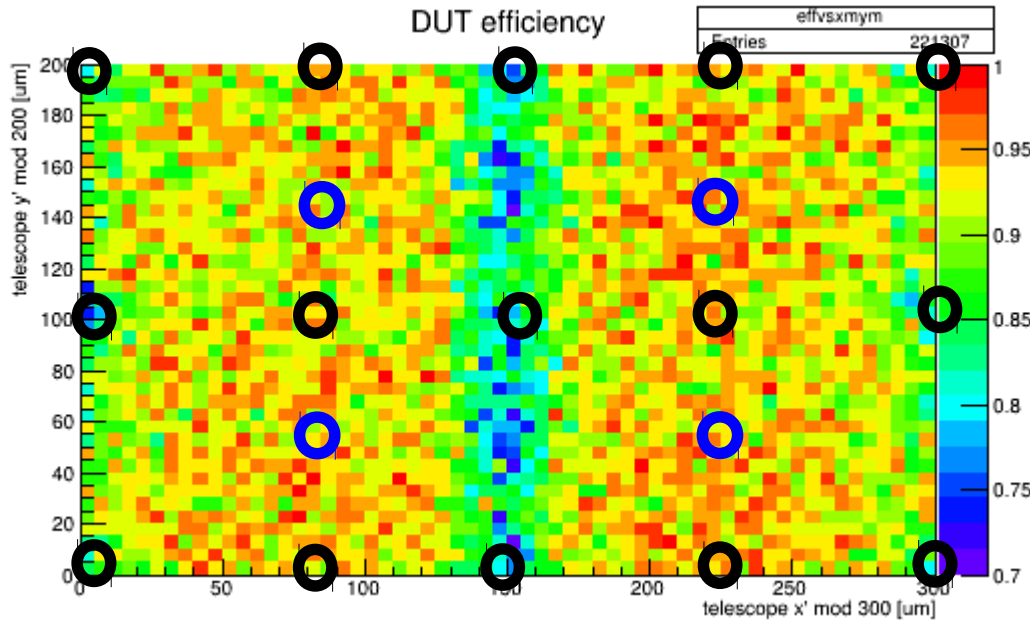
$V_{bias} = 140$ V

$T = -15$ °C



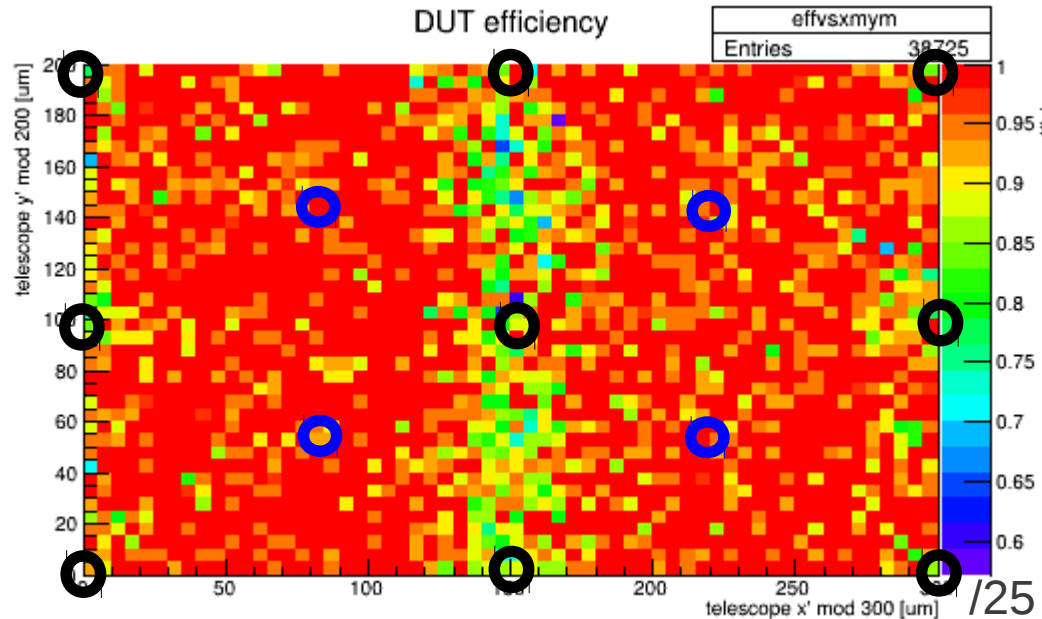
TEST BEAM RESULTS.

Irradiated sensors ($10^{15} n_{eq}/cm^2$).



↑
DENSE

→
SPARSE



PRELIMINARY
140 V
T = - 15 °C

CONCLUSIONS:

* Electrical characterization

Sensor biasing through the bias ring and by Punch through are in a good agreement

* ^{90}Sr Characterization

- Sensors show a good performance up to $5 \cdot 10^{15}$ neq/cm²
- Operation voltage below 200V
- These results are compatible with those from IBL (ATLAS)

* Test Beam

- Unirradiated Dense pattern show a more homogeneous performance in terms of efficiency.
 - Irradiated samples charge distributions under study.
- Pulse High Calibration performance.
- Efficiency maps in irradiated samples. V_{FD} ?

THANK YOU FOR YOUR ATTENTION!

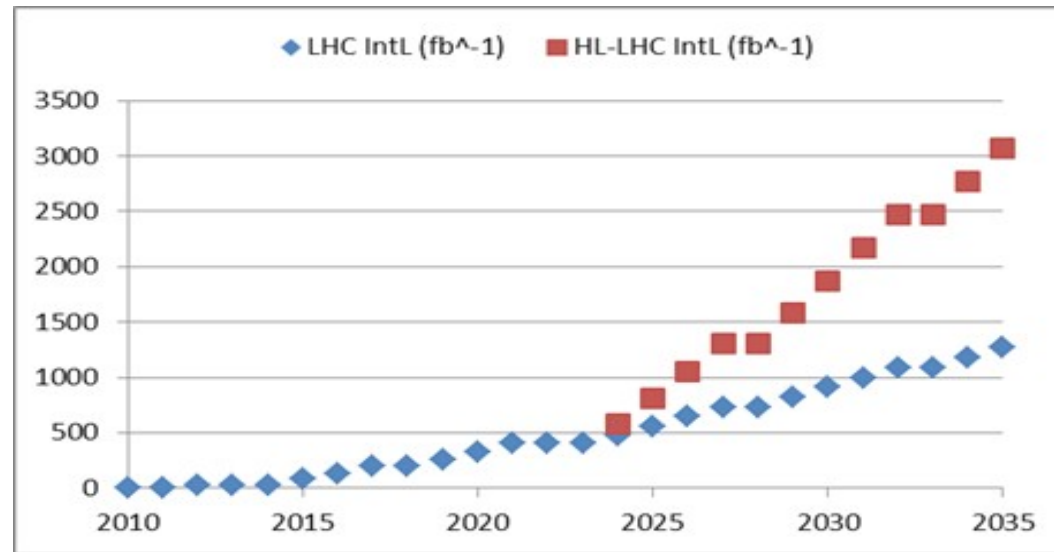
Acknowledgements:

- PSI, ETH and DESY – CMS pixel teams
- Specially
 - Hans Christian kaetsli
 - Silvane Streuli
 - Andrey Starodumov
- KIT & LJ irradiation facilities
- AIDA telescope crew

Backup

Motivation

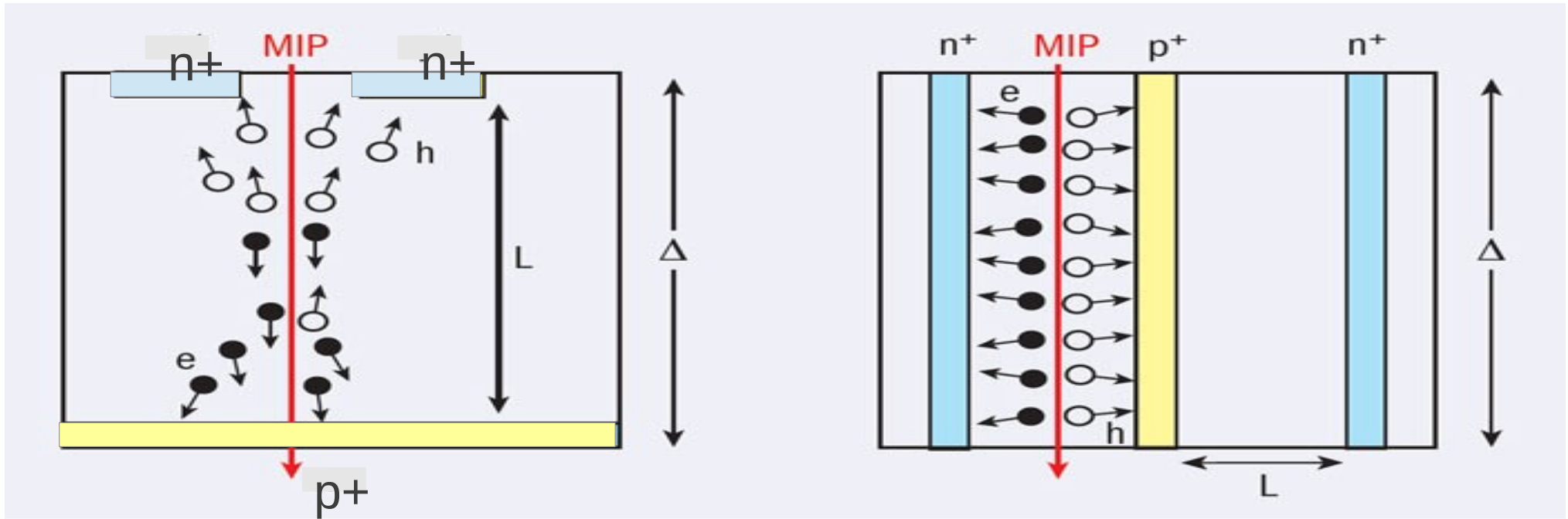
- LHC experiments are expected to undergo a constant increase of radiation levels, a possible HL-LHC scenario will get things tougher



- LHC Phase II vertex detectors must deal with fluences about $2 \cdot 10^{16}$ neq/cm²
- Here we are going to assess the radiation resistance of 3D double-sided pixel sensors in terms of:
 - Increase of the depletion voltage (V_{fd})
 - Reduction of the CCE
 - Tracking Performance and efficiency

Planar Pixel

3D Pixel



$$V_{FD} \propto L^2$$

3D Detectors Advantages

- Operational. Full depletion of the detector requires lower voltages
- Intrinsic. Shorter collection distances

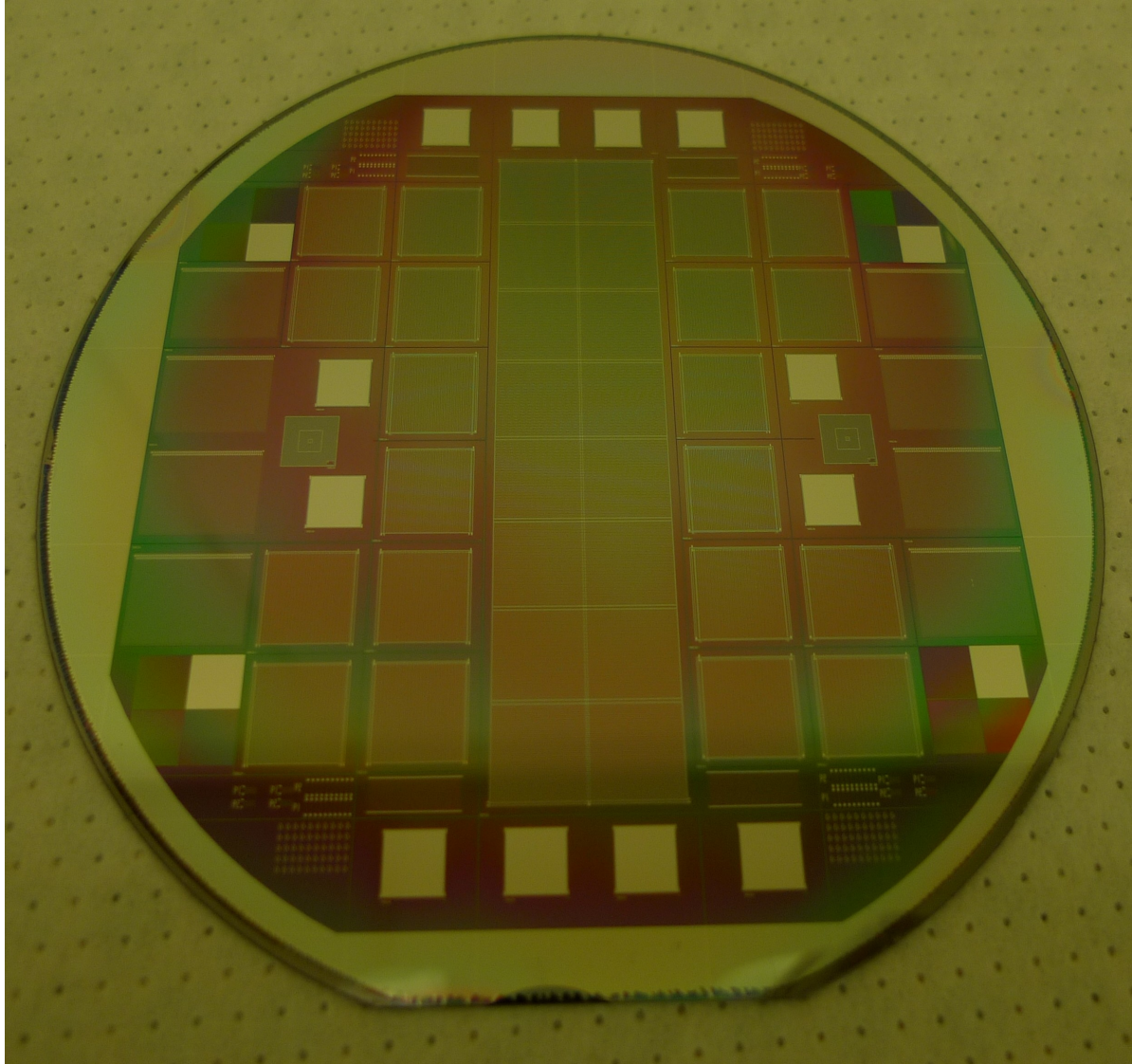
Depletion Area in 3D-Pixels

- Coaxial Symmetry
- r_1 is the electrode radius
- r_2 is the distance between columns
- The depletion voltage is the minimum voltage at which the bulk of the sensor is fully depleted

$$V_{fd} = \frac{1}{2} \frac{Nq}{\epsilon} \left[r_1^2 \ln\left(\frac{r_2}{r_1}\right) - \frac{1}{2} (r_2^2 - r_1^2) \right]$$

$$V_{fd} \text{ (coax)} = 0.9 \cdot V_{fd} \text{ (planar)}$$

CNM Production and Description



6 wafers:

Wafers 5,6,7,8:

- 285 μm thickness

Wafer 11:

-230 μm thickness

Wafer 3:

- 285 μm thickness

- Resistor bias grid

*** Each wafer includes:**

1 Full Module (8x2)

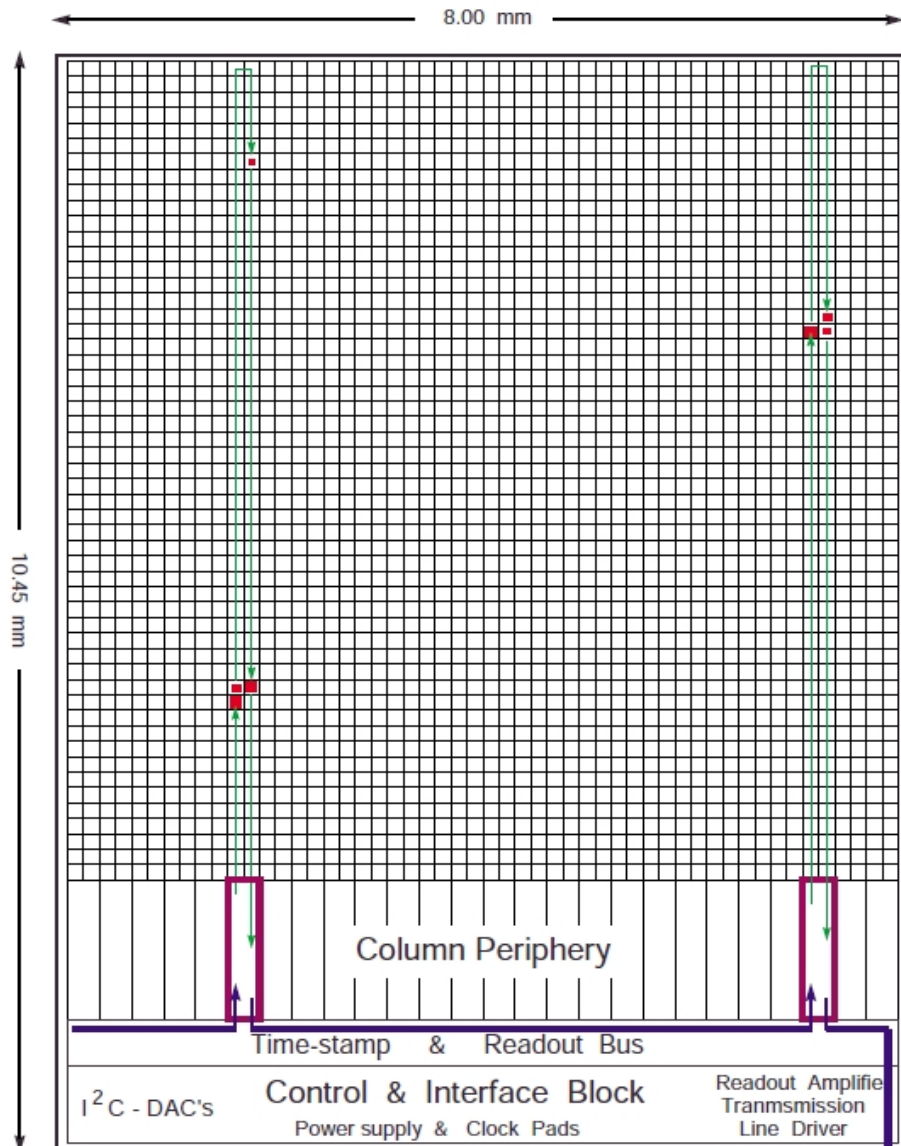
20 Single Chips

8 Strip sensors

12 Pads

Test structures

Readout Chip



- Paths of column token through double-column (green)
- Paths of the readout Token through the double- column peripheries
- When the column token stops at a pixel with hits. All hit information (pulse height, address...) is transferred To the column periphery where it is Stored in data buffer

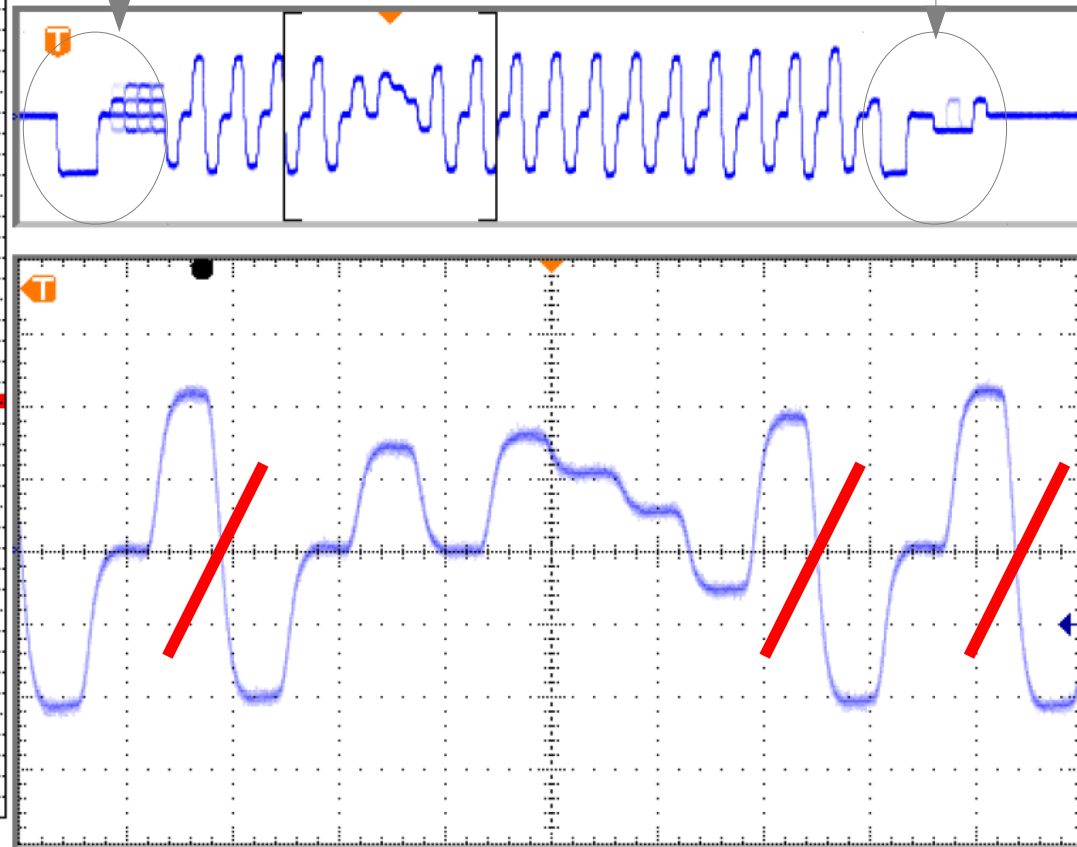
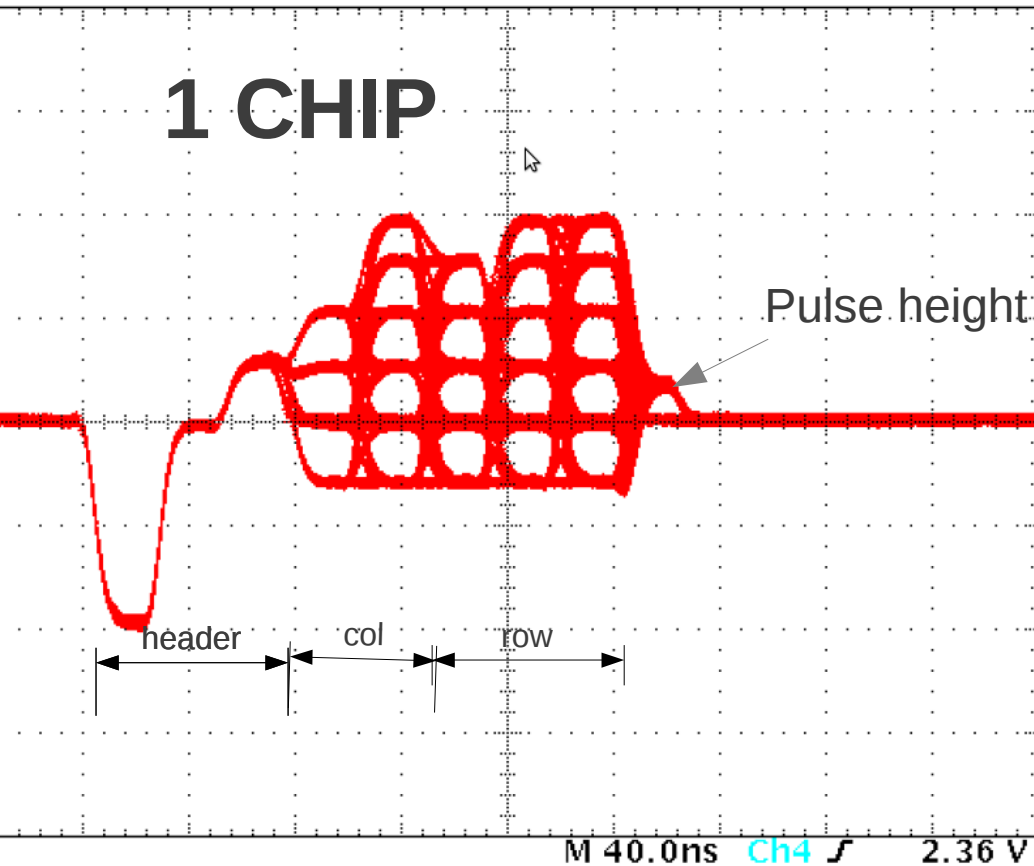
- Pixels without hits are skipped by the token
- Other double columns without hits for this Trigger are not affected and continue data acquisition

Readout format

TBM header within an event counter

TBM trailer

16 CHIPS



Chip 1,2,3,4--> no data

Chip 5--> 1 data

Chip 6--> no data

...

ROC QUALIFICATION

- **Calibrate Signal inputs**

- Vcal
- Vana
- Vthrc
- CalDel

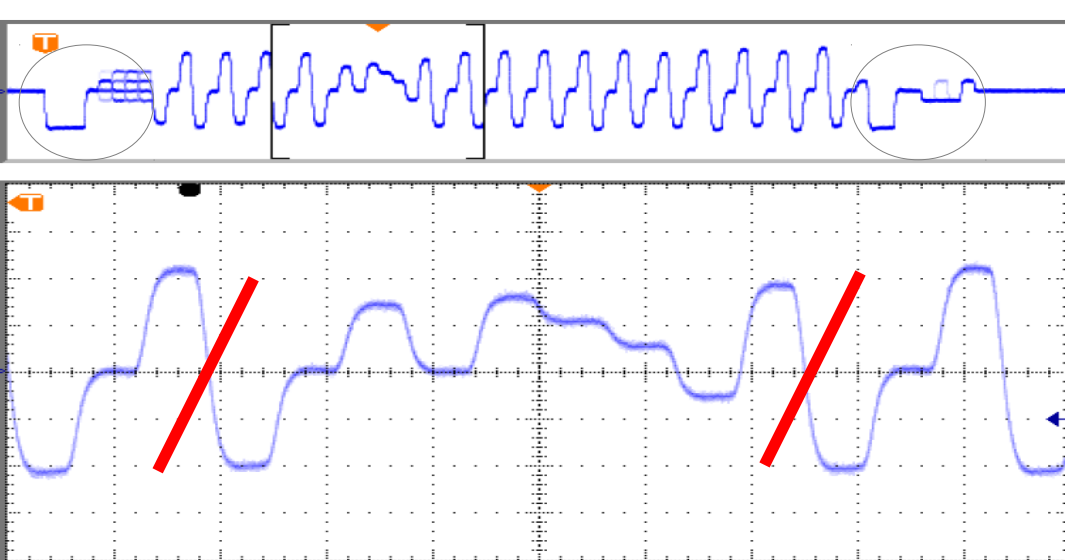
- **Pixel readout circuits**

- Pixel
- Trim bit
- Bump-Bonding
- Pixel Address

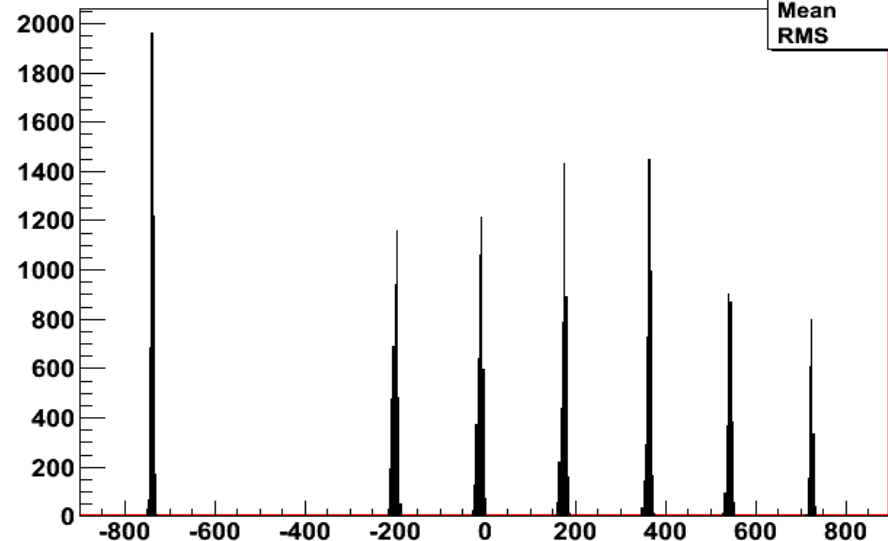
- **Functionality of the module**

- Noise
- Trimming
- Gain and Pedestal
- IV
- Thermal Cycle

Address levels and trimming

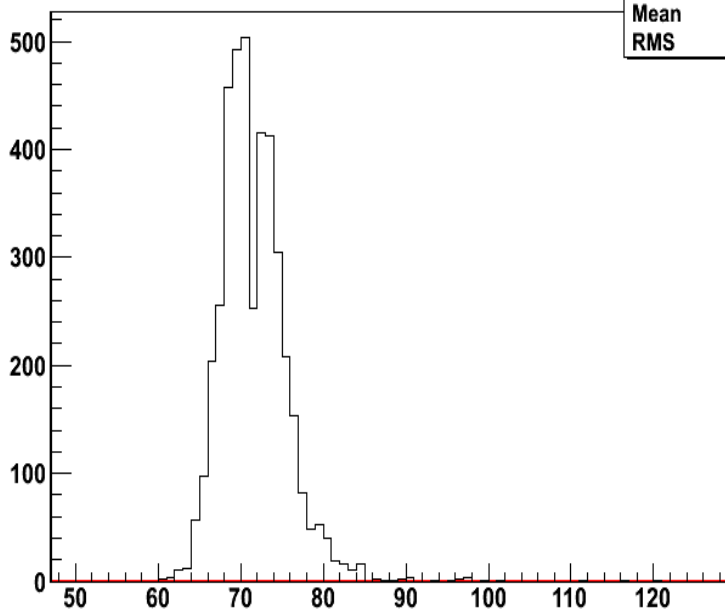


AddressLevels_C0



AddressLevels_C0	
Entries	4000
Mean	43.51
RMS	440.9

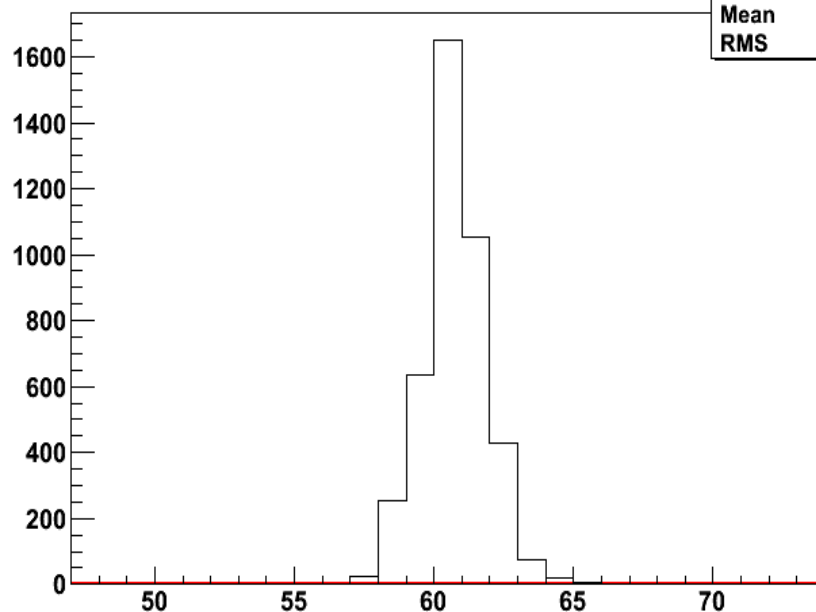
VcalThresholdMap_C0Distribution



VcalThresholdMap_C0Distribution	
Entries	4160
Mean	71.62
RMS	4.161

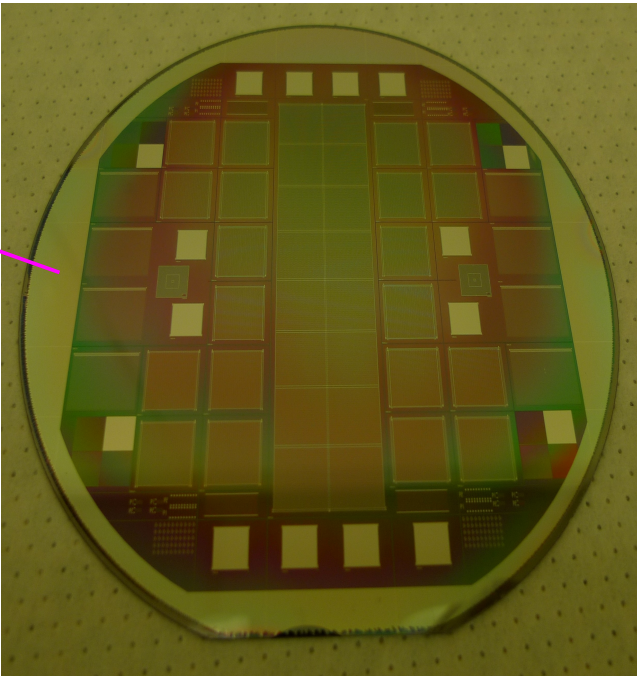
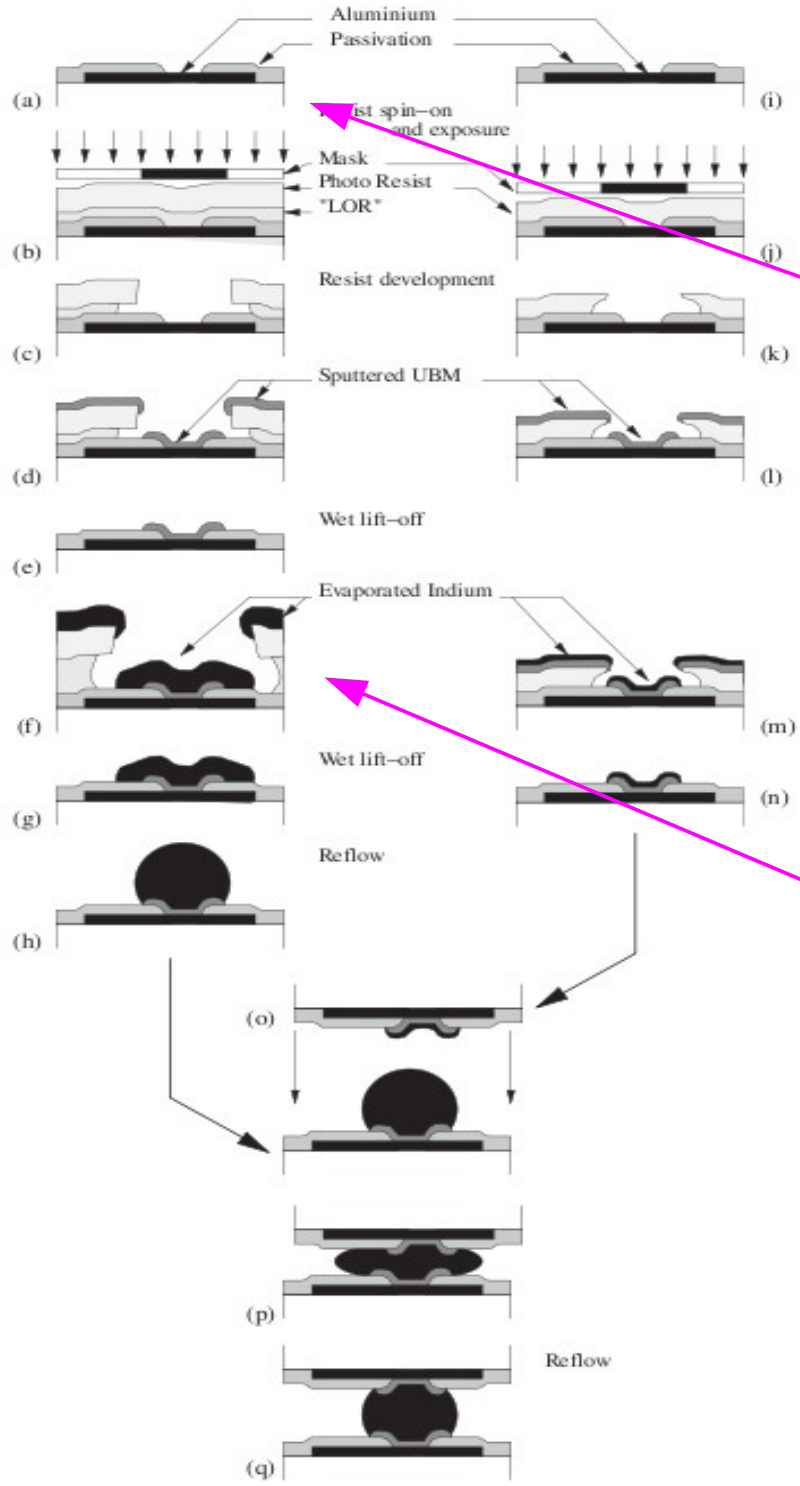


VcalThresholdMap_C0Distribution

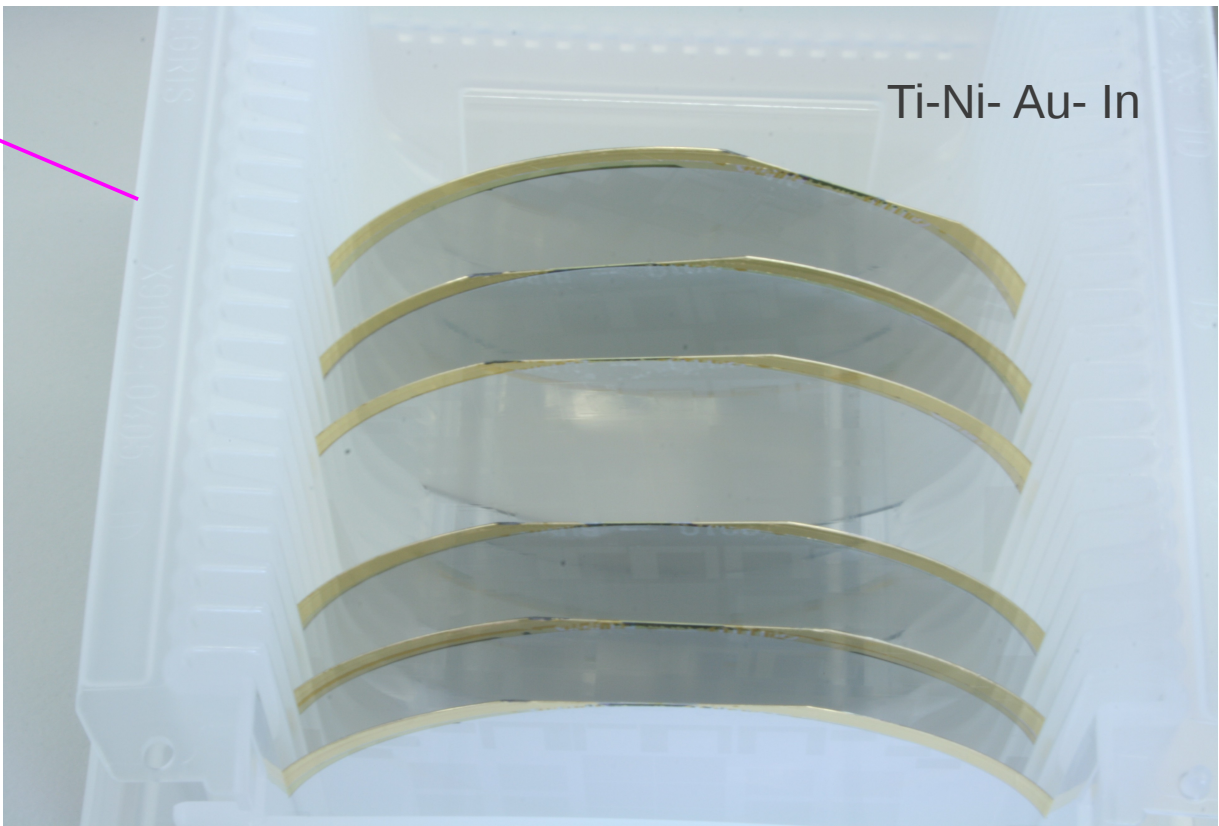


VcalThresholdMap_C0Distribution	
Entries	4160
Mean	60.76
RMS	1.199

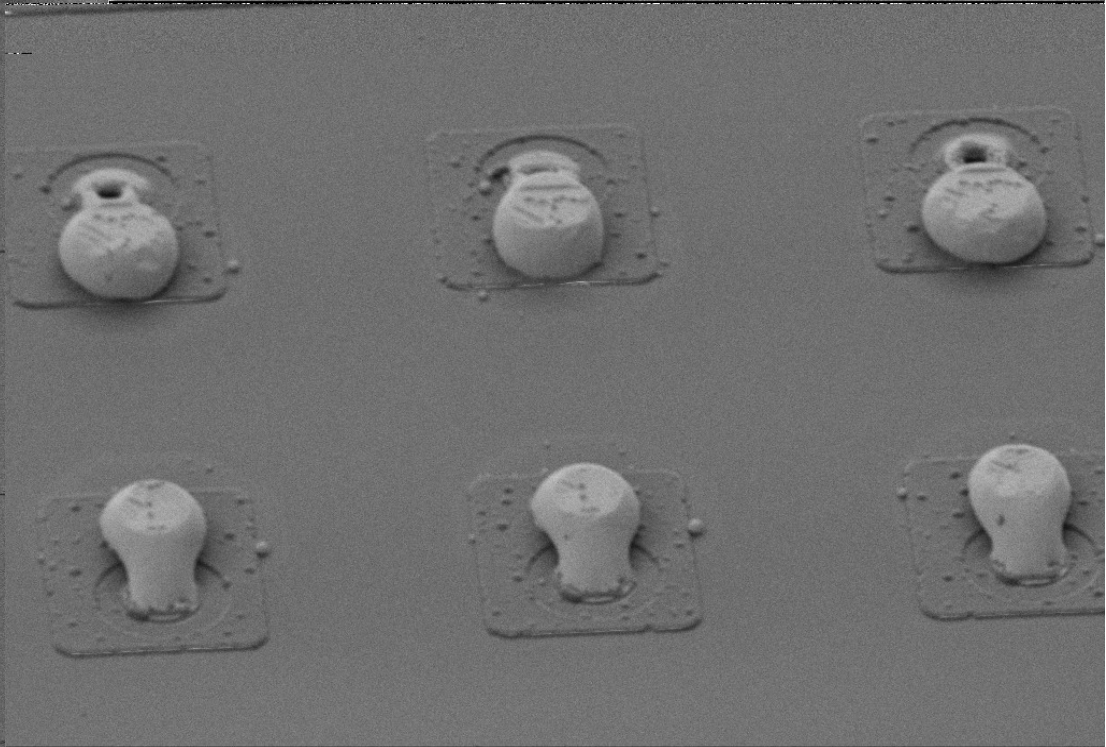
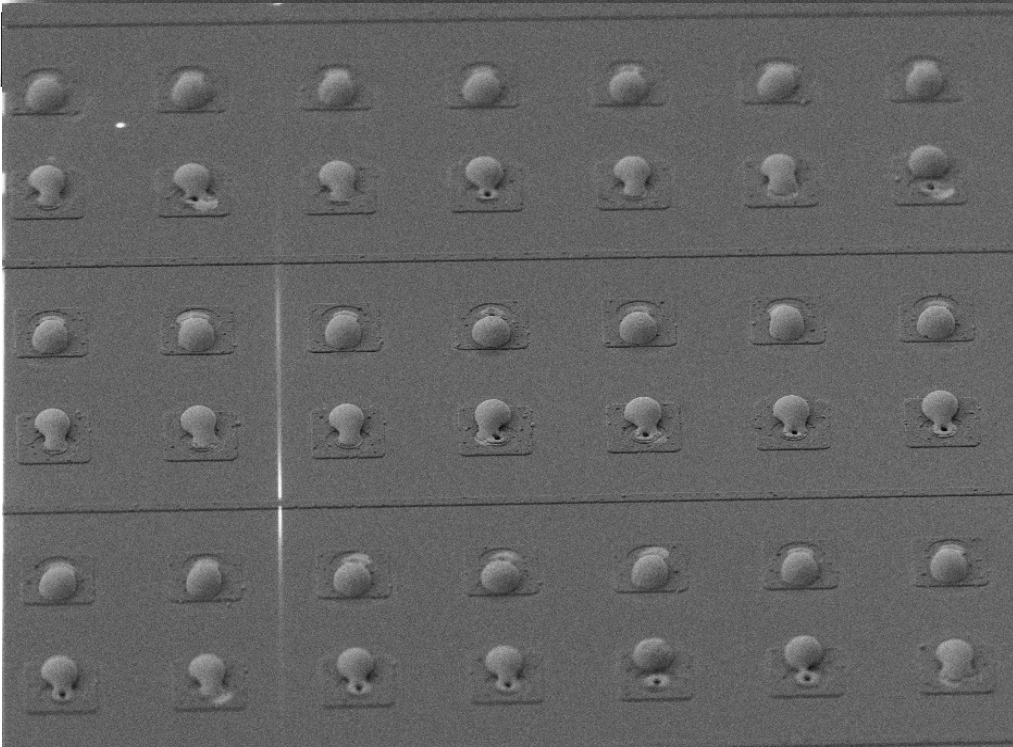
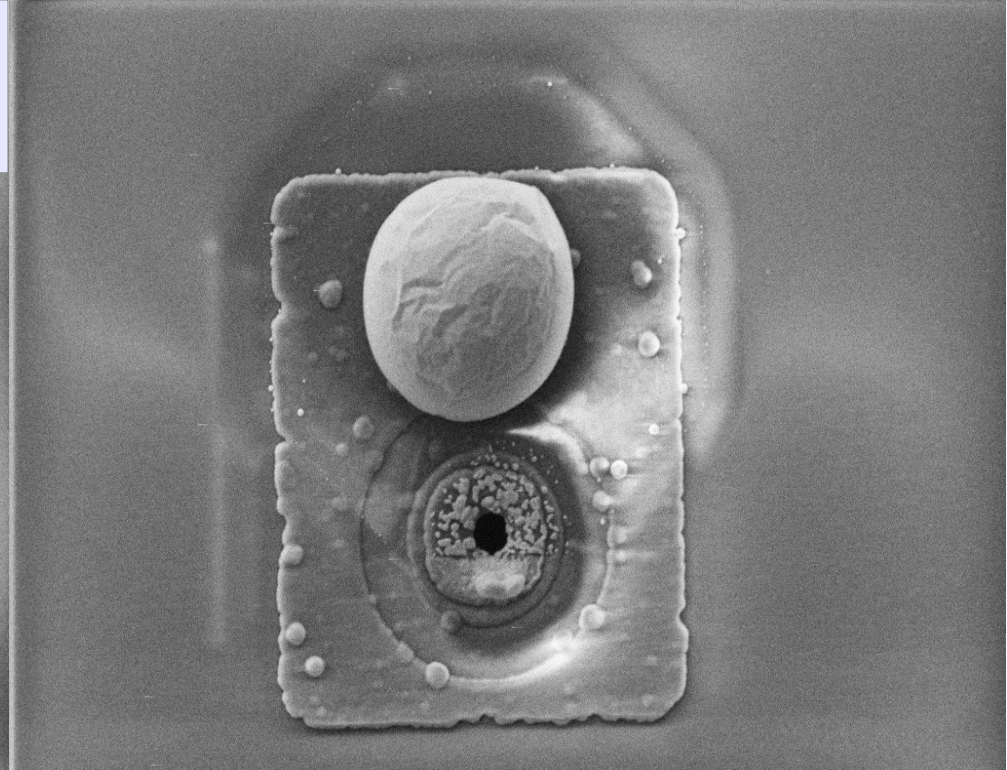
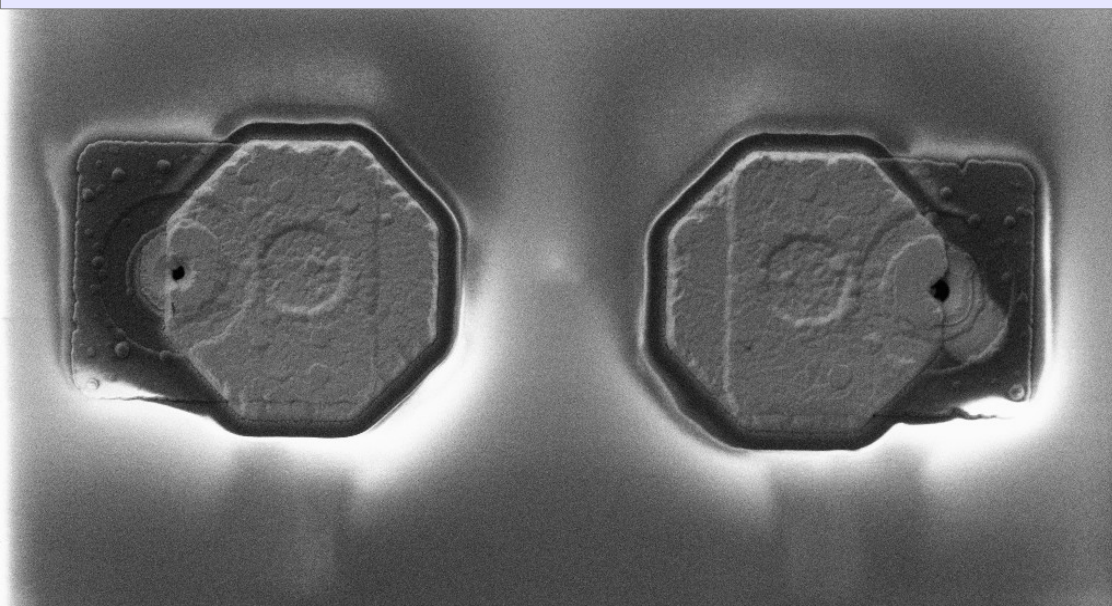
cisca Muñoz IFCA



Bump bonding



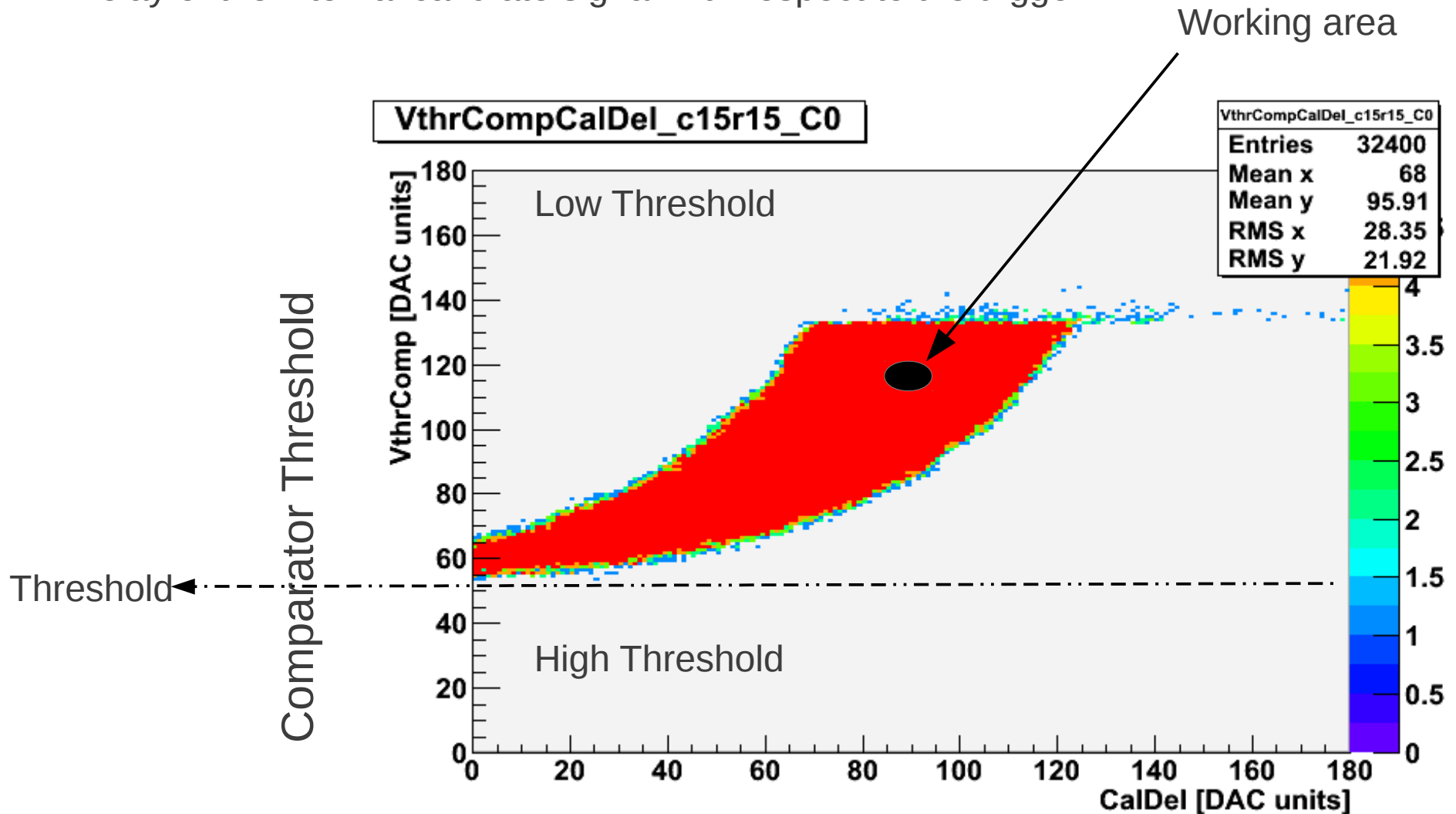
Scanning electron
Microscope
SEM



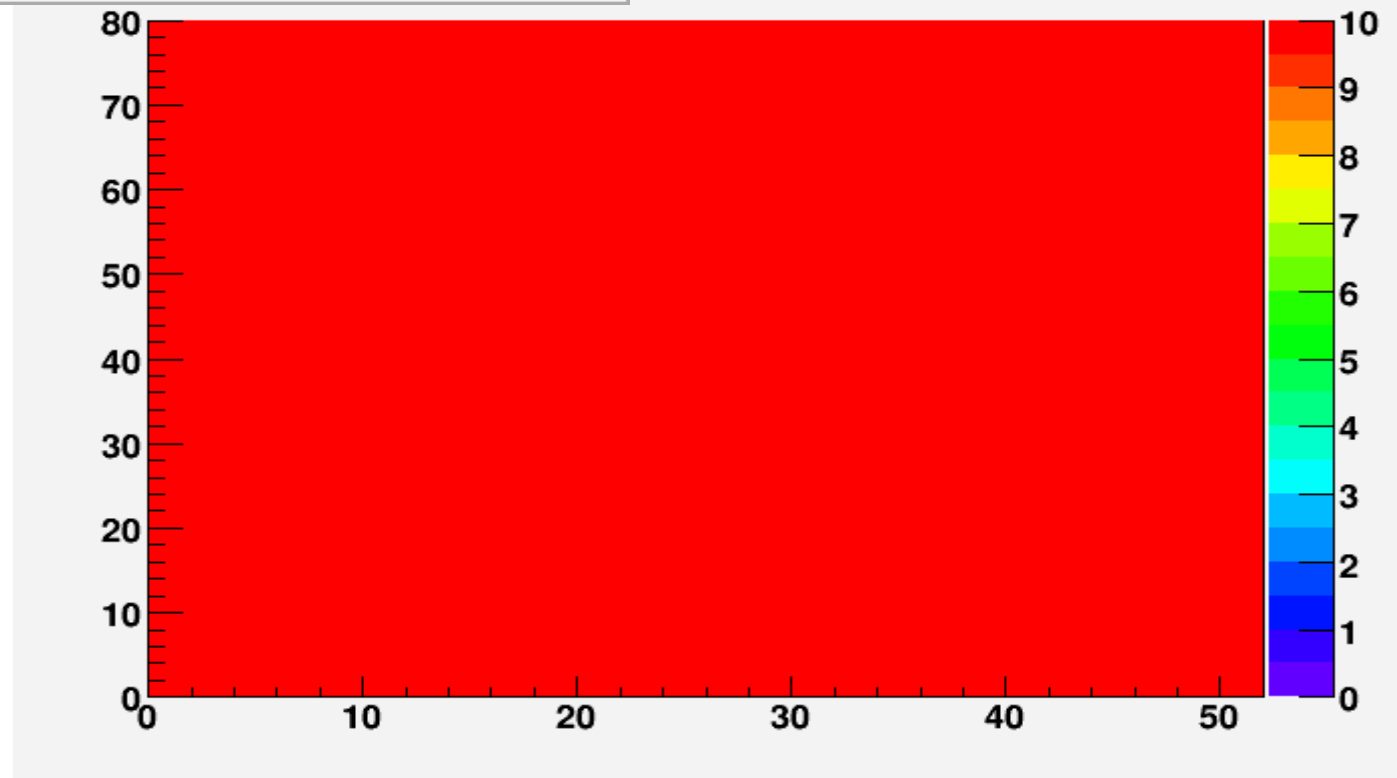
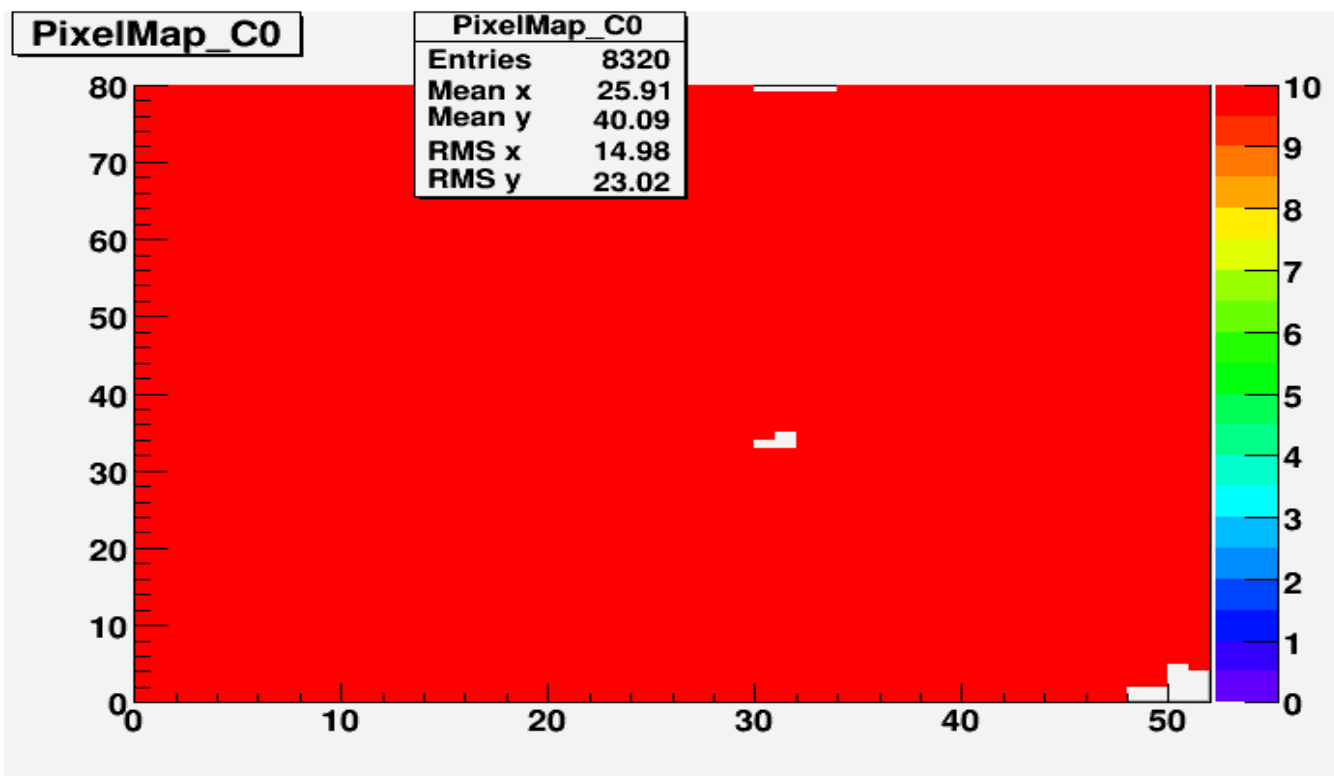
VthrComp vs CalDel

VthrComp → Injecting a signal with fixed amplitude (Vcal), finding the value at the comparator at which this signal is above threshold

CalDel → Delay of the internal calibrate signal with respect to the trigger



Pixel test

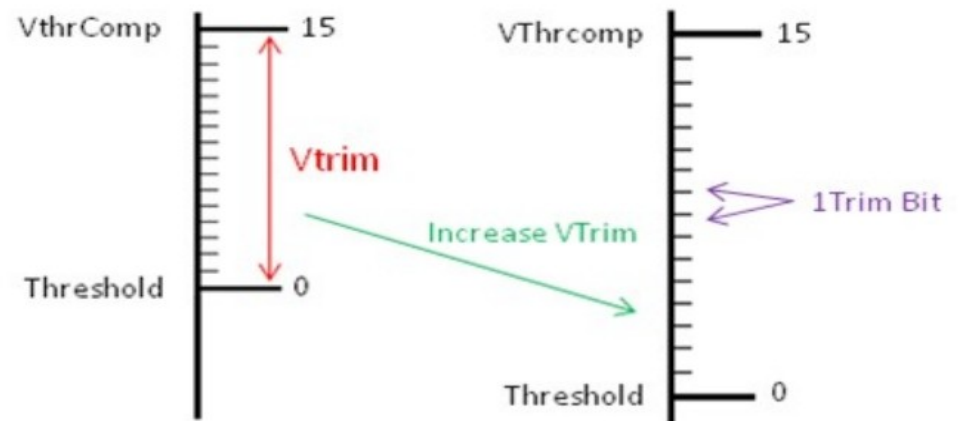




VthrComp, Vtrim and the Trim Bits

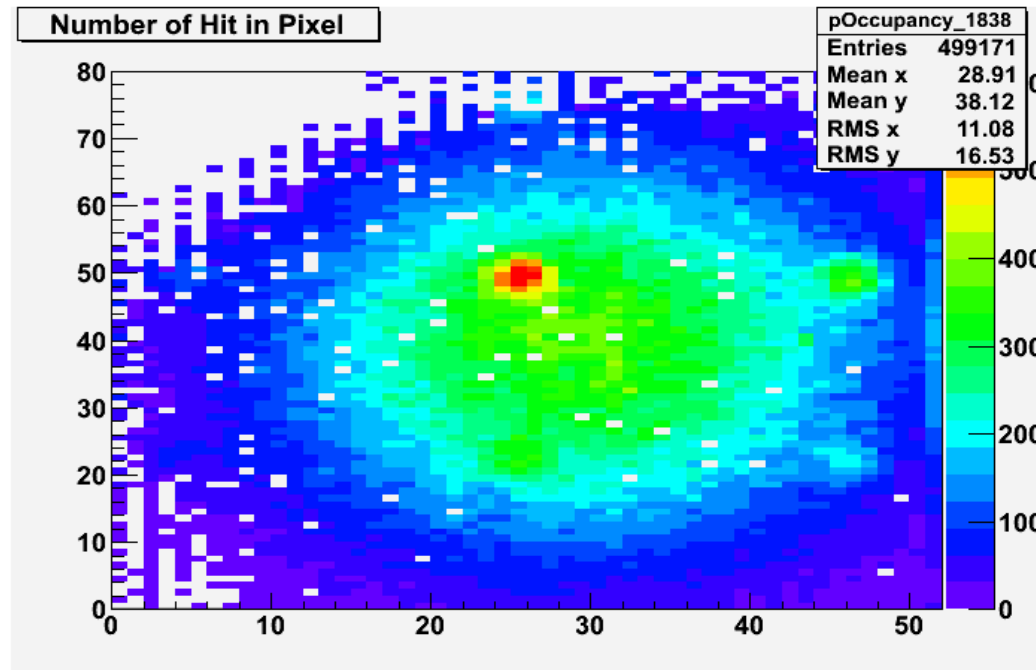


- These are the DAC's used to adjust the thresholds of the comparators of the PUC
- VthrComp adjusts the threshold for every pixel on the ROC
- Vtrim sets range of thresholds the trim bits can be used to program the PUC to have
- Higher VthrComp and Vtrim translates into lower thresholds
- Trim Bits of 0 gives the lowest possible threshold for a given VthrComp and Vtrim
- Increasing Vtrim gives more range of threshold, yes it increases the step size of a trim bit
- The goal of setting Vtrim and the trim bits is to make up for the small differences in transistors due to limitations of IBM process used to manufacture the ROC
- These differences vary from pixel to pixel, and it is important to have the same threshold across the entire ROC



Bump bonding. Interconnection process

- Bum bonding yield test
- Using a ^{90}Sr radioactive source
- An uniform pattern has been observed. Including the holes on the PCB (between sensor and scintillator)

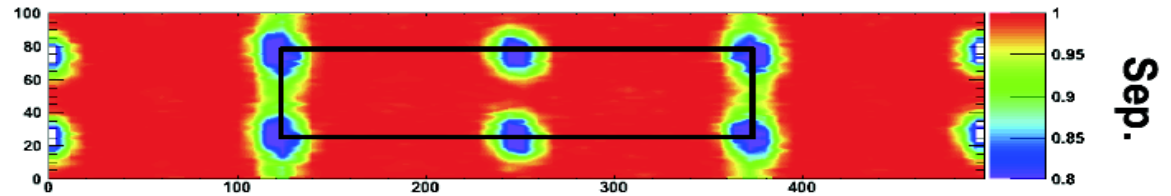


Latest results. IBL-ATLAS

Test-beam Results: planar and 3D

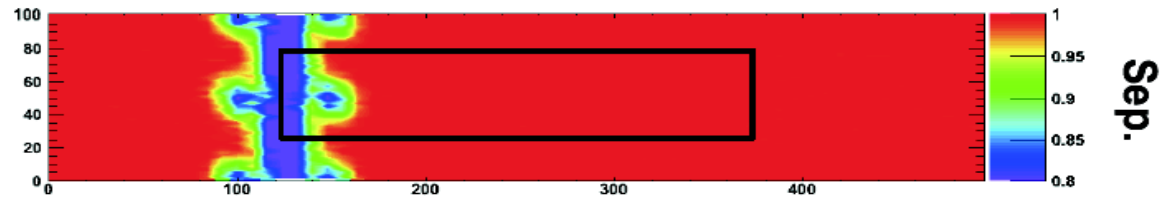
CNM-81 (3D),
 $5 \cdot 10^{15}$ n-irrad,

HV=160V
Eff=97.46



LUB4 (Planar),
 $5 \cdot 10^{15}$ n-irrad,

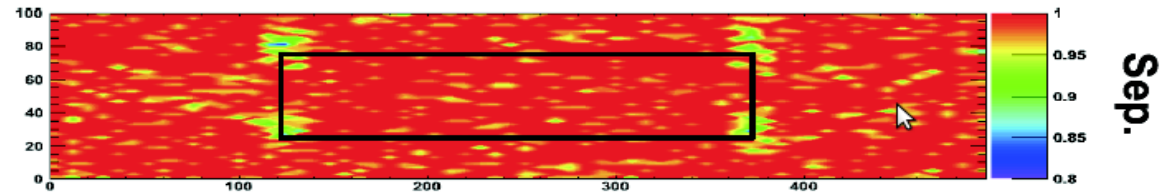
HV=1000V
Eff=97.90



Batch4, 0 degree (B.E. = 80 GeV)

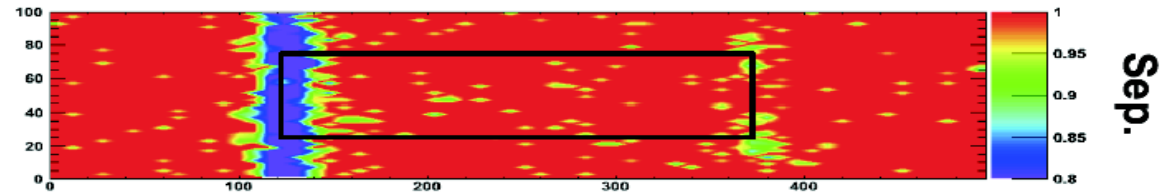
SCC34 (CNM-3D),
 $5 \cdot 10^{15}$ p-irrad,

HV=160V
Eff=98.96



SCC60 (Planar),
 $5 \cdot 10^{15}$ p-irrad,

HV=940V
Eff=97.65



Batch1, 15 degree (B.E. = 120 GeV)

23

Devices

Name	Qty	Description
CMS_MC	1	Large module, matrix 8x2 detectors, <u>sparse</u> pattern of P columns and <u>single</u> guard ring
CMS_SC_11	5	Single chip detector with <u>sparse</u> pattern of P columns and <u>single</u> guard ring
CMS_SC_12	5	Single chip detector with <u>sparse</u> pattern of P columns and <u>double</u> guard ring
CMS_SC_21	5	Single chip detector with <u>dense</u> pattern of P columns and <u>single</u> guard ring
CMS_SC_22	5	Single chip detector with <u>dense</u> pattern of P columns and <u>double</u> guard ring
3D-Strip detector (6)	8	3D-strip detectors with 128 strips of 80 μm pitch, 15 μm strip width and single guard ring
3D-Pad detector (7)	12	3D-pad detector with single guard ring
Test structures	-	Layer deposition test, polysilicon resistance test, hole alignment test